Forum for Electromagnetic Research Methods and Application Technologies (FERMAT)

Small and Wideband Patch Antennas and Planar Microwave Circuits for Wireless and Biomedical Applications

Dr. Yongxin Guo, Associate Professor
Department of Electrical and Computer Engineering
Email: eleguoyx@nus.edu.sg
11 January 2016

 1

Abstract/Keywords

Abstract: In this presentation, the recent research activities on "**Small and Wideband Patch Antennas and Planar Microwave Circuits for Wireless and Biomedical Applications**" conducted by the research group led by Associate Professor Yongxin Guo at the Department of Electrical and Computer Engineering, National University of Singapore will be reported.

The topics on "**Antennas and Wireless Power for Biomedical Applications**" has received a lot of attention. On-body antennas for wearable applications and In-body antennas for bio-implants will be presented first. Wireless power and energy harvesting have become more important to enable bio-telemetry. In addition to the traditional inductive near-field wireless power, capacitive wireless power and far-field wireless power will also be addressed. In the meantime, effort has been made to improve the dynamic range of the rectifier circuit for the energy harvesting, especially for low-power scenarios.

The topic on "**Small and Wideband Patch Antennas**" has been focused previously. The wideband L-probe feeding technique will be introduced here. In the meantime, wideband patch antennas with broadband feeding networks will be presented. The antenna performance can be improved significantly in a wide bandwidth with the proposed broadband feeding networks. Various wideband millimeter-wave antennas-in-package and on-chip antennas will also be reported for future system in package applications since antennas are small in size at higher frequencies.

"MMIC modeling and design" is another topic we are put effort on as it is crucial to develop high-density integrated transceivers for wireless and biomedical applications. It is believed that developing high-density integrated transceiver technologies for wireless and biomedical applications will attract more interests.

Keywords: Wideband patch antennas, small antennas, wearable antennas, implantable antennas, antennas in package, on-chip antennas, wideband feeding networks, wireless power, inductive wireless power, capacitive wireless power, far-field wireless power, RF energy harvesting, MMIC, LTCC.

Briefbio

Dr Yong Xin Guo joined the Department of Electrical and Computer Engineering, National University of Singapore (NUS), as an Assistant Professor in February 2009 and was promoted to an Associate Professor with tenure in Jan 2013. He received the B.Eng. and M.Eng. degrees from Nanjing University of Science and Technology, Nanjing, China, and the Ph.D. degree from City University of Hong Kong, all in electronic engineering, in 1992, 1995 and 2001, respectively. From September 2001 to January 2009, he was with the Institute for Infocomm Research, Singapore, as a Research Scientist.

He has authored or co-authored 171 international journal papers and 176 international conference papers. Thus far, his publications have been cited by others more than 2086 times and the H-index is 28 (source: Scopus). He holds one Chinese Patent, one U.S. patent and one filed PCT patent. His current research interests include small and wideband patch antennas, implantable/wearable antennas, on-chip antennas and antennas in package, RF energy harvesting and wireless power, MMIC modeling and design, etc..

Dr Guo was General Chairs and TPC Chair for a few IEEE conferences. He is serving as Associate Editors for the IEEE Antennas and Wireless Propagation Letters (AWPL), IET Microwaves, Antennas & Propagation and Electronics Letters. He was a recipient of the Young Investigator Award 2009, National University of Singapore. He received 2013 Raj Mittra Travel Grant Senior Researcher Award. He received the Best Poster Award in 2014 International Conference on Wearable & Implantable Body Sensor Networks (BSN 2014), Zurich, Switzerland. He is a co-recipient of of Design Contest Award of the 20th International Symposium on Low Power Electronics and design (ISLPED), Rome, Italy, July 2015. His PhD students received Best Student Paper Awards from IEEE MTT-S IMWS-Bio 2015 in Taiwan, IEEE iWEM 2013 in Hong Kong, 2011 National Microwave and Millimeter-Wave Conference at Qingdao, China and IEEE ICMMT 2010 in Chengdu, China.

Research Areas

High-Density Integrated Transceiver Technologies for Wireless and Biomedical Applications

MIC / MMIC
- Microwave and millimetre-wave MIC/MMIC design
- Microwave semiconductor device modelling and characterization
- LTCC based System-in-package technology

EM / Antenna
- (1) Wideband antennas; (2) multiband antennas; (3) small antennas; (4) Tunable antennas; (5) New material antennas
- (1) LTCC on-package antennas; (2) CMOS on-chip antennas
- (1) Wearable and Implanted antennas; (2) Inductive power transmission for implants; (3) In-body and on-body channel modeling; (4) Heating and SAR for implanted devices.

RF Energy Harvesting

Outline

	Research Topics	Pages
Primary Area: Small and Wideband Planar Antennas	Small Wideband On-body/In-Body Antennas	07-22
	Wireless Power and RF energy harvesting	23-50
	Wideband patch antennas	51-55
	Wideband Patch Antennas with Broadband Feeding Networks	56-67
	Small Wideband and Multiband Planar Antennas	68-72
	Wideband Millimeter-Wave In-Package/On-Chip Antennas	73-140
Secondary Area: Microwave circuits	MMIC modeling and design	141-155
	Advanced passive devices	156-165

Lab Facilities

 6

On-/In-Body Antennas for Bio-Medical and Healthcare

Demand for utilization of wireless telemetry systems in medicine has recently significantly increased due to needs for early diagnosis of diseases and continuous monitoring of physiological parameters.

Small Wideband On-body/In-Body Antennas

1. C.R. Liu, Y.X. Guo, X.G. Liu, S.Q. Xiao, An Integrated On-chip Implantable Antenna in 0.18μm CMOS Technology for Biomedical Applications, accepted by IEEE Transactions on Antennas and Propagation.
2. C.R. Liu, Y.X. Guo, S.Q, Xiao, A review of implantable antennas for wireless biomedical devices, Forum for Electromagnetic Research methods and Application Technologies (FERMAT), 2016.
3. W. Lei, Y.X. Guo, Miniaturized differentially fed dual-band implantable antenna: Design, realization and in vitro test, Radio Science, 10.1002/2014RS005640, pp. 959-967, 2015
4. L.J. Xu, Y.X. Guo, W. Wu, Miniaturized Circularly Polarized loop Antenna for Biomedical Applications, IEEE Transactions on Antennas and Propagation, vol. 63, no.3, pp. 922-930, March 2015.
5. C.R. Liu, Y.X. Guo, S.Q. Xiao, Circularly Polarized Helical Antenna for ISM-Band Ingestible Capsule Endoscope Systems, IEEE Transactions on Antennas and Propagation, vol.62, no.12, pp. 6027-6039, Dec 2014.
6. C.R. Liu, Y.X. Guo, S.Q. Xiao, Capacitively Loaded Circularly Polarized Implantable Patch Antenna for ISM-Band Biomedical Applications, IEEE Transactions on Antennas and Propagation, vol. 62, no.5, pp. 2407-2417, May 2014.
7. Z. Duan, Y.X. Guo, M. Je, and D.L. Kwong, Design and in vitro test of differentially fed dual-band implantable antenna operating at MICS and ISM bands, IEEE Transactions on Antennas and Propagation, vol. 62, no.5, pp. 2430-2439, May 2014.
8. Z.G. Liu, Y.X. Guo, Dual-band low profile patch antenna for body centric communications, IEEE Transactions on Antennas and Propagation, April 2013.
9. Z. Duan, Y.X. Guo, R.F. Xue, M. Je, and D.L. Kwong, Differentially-fed dual-band implantable antenna for biomedical applications, IEEE Transactions on Antennas and Propagation, Dec 2012.
10. Z.G. Liu, Y.X. Guo, Compact Low-Profile Dual Band Metamaterial antenna for body centric communications, IEEE Antennas and Wireless Propagation Letters, vol. 14, pp. 863-866, 2015.
11. L.J. Xu, Y.X. Guo, W. Wu, Bandwidth Enhancement of An Implantable Antenna, IEEE Antennas and Wireless Propagation Letters, vol. 14, pp. 1510-1513, 2015.
12. L.J. Xu, Y.X. Guo, W. Wu, Miniaturized Dual-Band Antenna for Implantable Wireless Communications, IEEE Antennas and Wireless Propagation Letters, vol. 13, pp. 1160-1163, 2014.
13. L.J. Xu, Y.X. Guo, W. Wu, Miniaturized slot antenna for biomedical applications, Electronics Letters, vol. 49, no. 17, Aug 2013.
14. L.J. Xu, Y.X. Guo, W. Wu, Dual-Band Implantable Antenna with Open-End Slots in Ground, IEEE Antennas and Wireless Propagation Letters, vol. 11, pp. 1568-1571, 2012.
15. C.R. Liu, Y.X. Guo, S.Q. Xiao, Compact Dual-Band Antenna for Implantable Devices, IEEE Antennas and Wireless Propagation Letters, vol. 11, pp. 1508-1511, 2012.
16. C.R. Liu, Y.X. Guo, S.Q. Xiao, A Hybrid Patch/Slot Implantable Antenna for Biotelemetry Devices, IEEE Antennas and Wireless Propagation Letters, 2012
17. C.R. Liu, S.Q. Xiao, et al, Compact circularly-polarised microstrip antenna with symmetric-slit, Electronics Lett, vol. 48, no.4, pp. 195-196, 2012.

Wireless Medical Communications

- The ageing population poses many challenges to healthcare systems, especially on chronic illness management. Early warning systems using body sensor networks are necessary for human health.
- There is a need for cable clutter to be reduced in the hospital setting. Wearable and wireless biosensors can address this need.

Commercially available

Philips wearable sensors (no wireless)

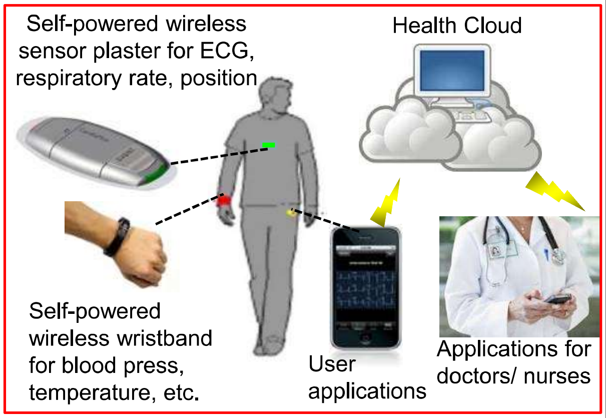

 9

Wireless Implantable Neuroprobe Microsystems

- A potential treatment for paralysis (e.g. tetraplegia) is to route control signals from the brain around the injury. Such signals could control electrical stimulation of muscles and restore movement of paralyzed limbs.

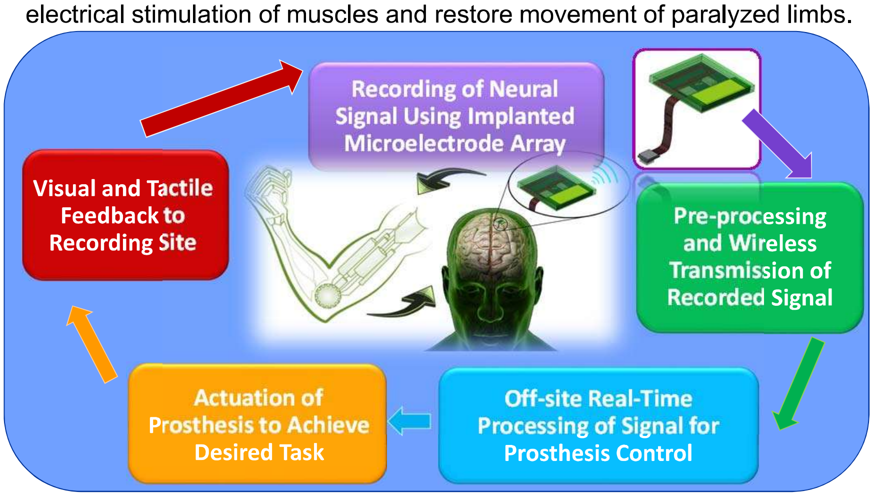

 10

Peripheral Nerve Prothesis

• The signal from the injured nerve can be detected and decoded, and then transmitted to stimulating electrodes implanted in multiple target muscles to restore **dexterous hand function** after nerve injury.

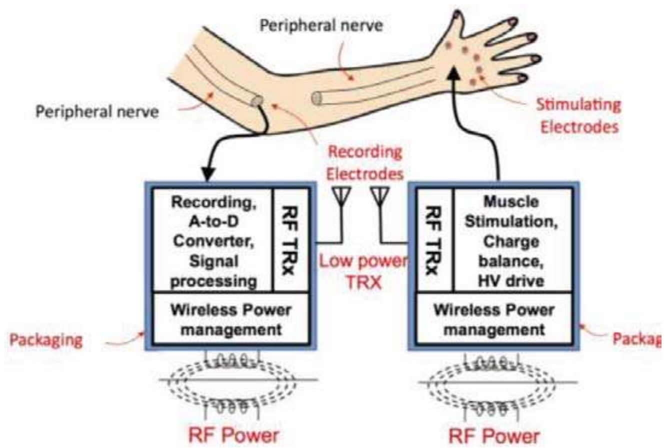

11

Capsule Endoscopy

- **Capsule endoscopy** is a way to record images of the digestive tract for use in medicine. The capsule is the size and shape of a pill and contains a tiny camera. After a patient swallows the capsule, it takes pictures of the inside of the gastrointestinal tract. The primary use of capsule endoscopy is to examine areas of the small intestine that cannot be seen by other types of endoscopy such as colonoscopy or esophagogastroduodenoscopy (EGD).

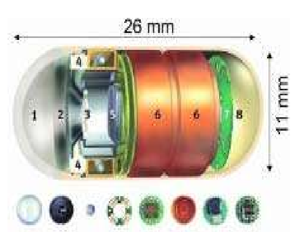

 12

Implanted Antennas

- Efficient implantable antennas are crucial to establish the reliable wireless link in the communications between the implants and the external devices or between wearable devices and external devices.

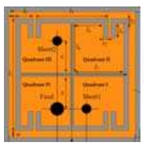
[1]
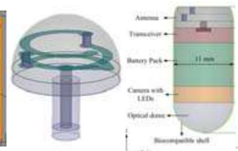
[2]
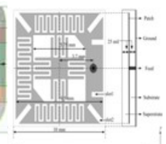
[3]

[4]
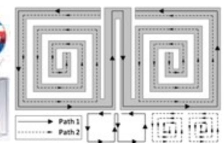
[5]

1. L.J. Xu, Y.X. Guo, W. Wu, Miniaturized Circularly Polarized loop Antenna for Biomedical Applications, IEEE Transactions on Antennas and Propagation, vol. 63, no.3, pp. 922-930, March 2015.
2. C.R. Liu, Y.X. Guo, S.Q. Xiao, Circularly Polarized Helical Antenna for ISM-Band Ingestible Capsule Endoscope Systems, IEEE Transactions on Antennas and Propagation, vol.62, no.12, pp. 6027-6039, Dec 2014.
3. C.R. Liu, Y.X. Guo, S.Q. Xiao, Capacitively Loaded Circularly Polarized Implantable Patch Antenna for ISM-Band Biomedical Applications, IEEE Transactions on Antennas and Propagation, vol. 62, no.5, pp. 2407-2417, May 2014.
4. Z. Duan, Y.X. Guo, M. Je, and D.L. Kwong, Design and in vitro test of differentially fed dual-band implantable antenna operating at MICS and ISM bands, IEEE Transactions on Antennas and Propagation, vol. 62, no.5, pp. 2430-2439, May 2014.
5. Z. Duan, Y.X. Guo, R.F. Xue, M. Je, and D.L. Kwong, Differentially-fed dual-band implantable antenna for biomedical applications, IEEE Transactions on Antennas and Propagation, Dec 2012.

 13

Printing Technology for On-Body Antennas

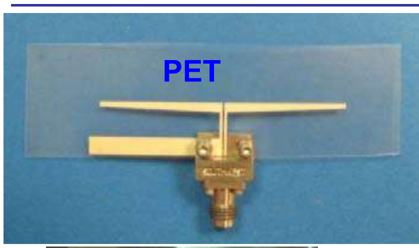

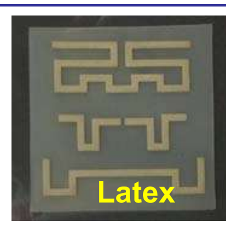

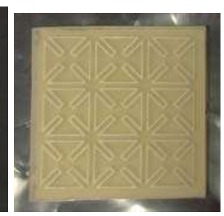
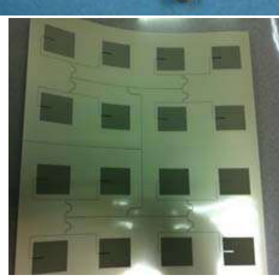


Z.G. Liu, Y.X. Guo, Dual-band low profile patch antenna for body centric communications, IEEE Transactions on Antennas and Propagation, April 2013. 14

Dual Band Metamaterial antenna for body centric communications

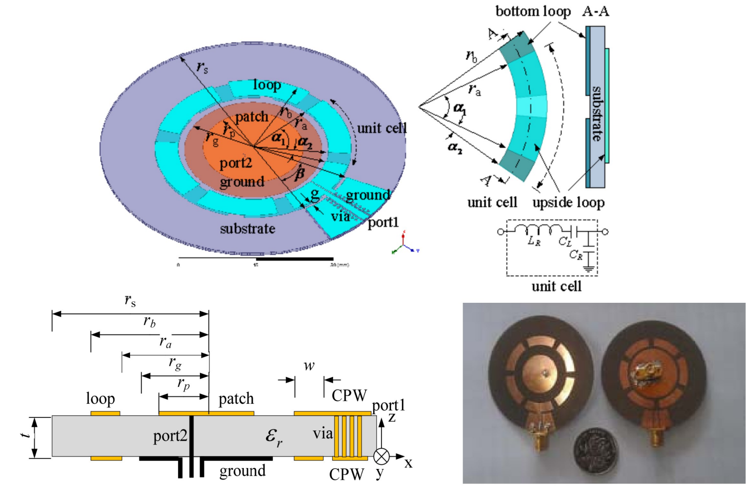

Z.G. Liu, Y.X. Guo, Compact Low-Profile Dual Band Metamaterial antenna for body centric communications, IEEE Antennas and Wireless Propagation Letters, vol. 14, pp. 863-866, 2015.

Dual Band Metamaterial antenna for body centric communications

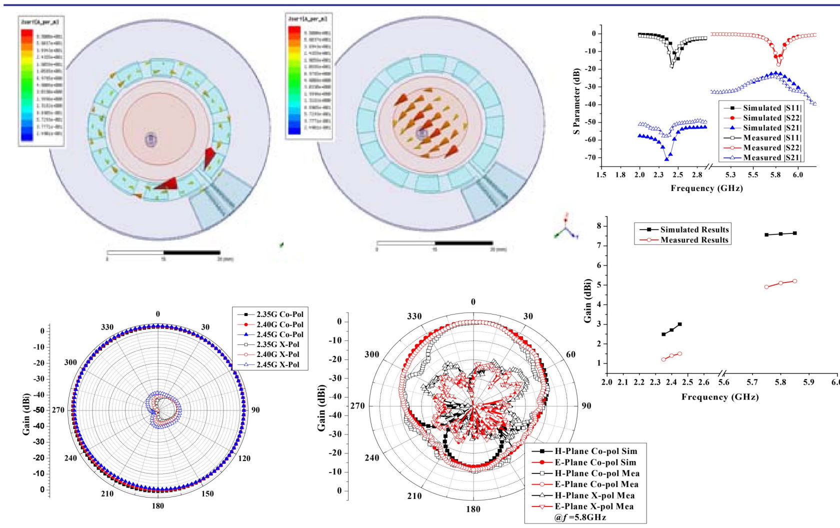

System block diagram and conceptual drawing of fully implantable wireless neural recording microsystem

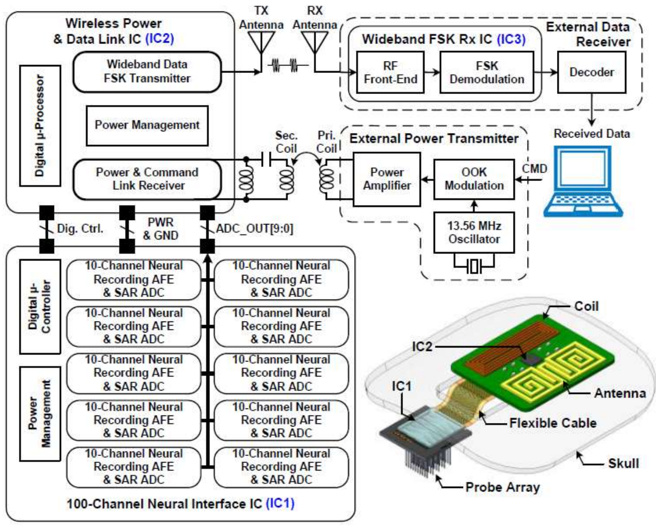

17

Implanted Differential Antennas

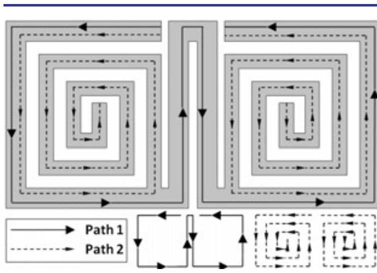

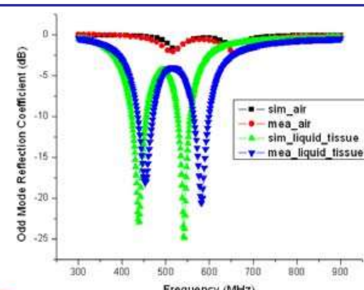

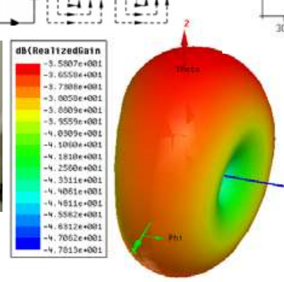

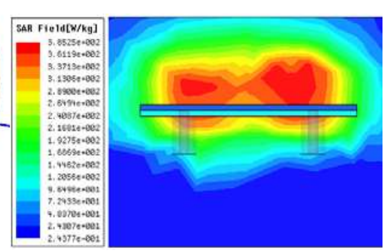

Z. Duan, Y.X. Guo, R.F. Xue, M. Je, and D.L. Kwong, Differentially-fed dual-band implantable antenna for biomedical applications, IEEE Transactions on Antennas and Propagation, Dec 2012.

18

Differential Implantable Antenna System tests

- System test Overview

The signal generator generates the clock of the transmitter, which is 13.56 MHz.

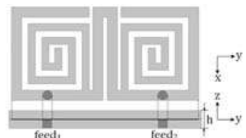

The FPGA board generates the data for transmission. The two frequencies of transmitter output are 433.92 MHz and 542.4 MHz. The transmitter is directly connected with the differential dual-band implantable antenna embedded in minced pork, eliminating the usage of baluns and matching circuits. The external half-wavelength dual-band dipole, which is spaced 20 mm apart from the implanted antenna, is connected with the signal analyzer.

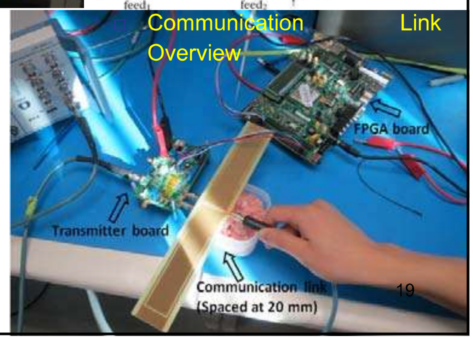

19

System tests

Screen snapshot of output power of the transmitter (around -23 dBm)

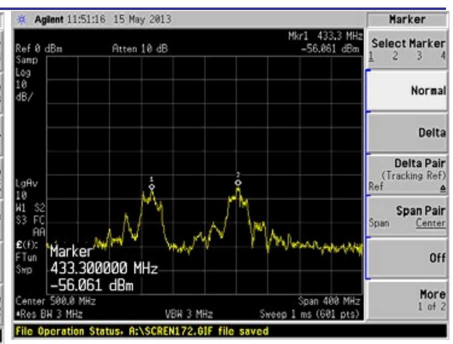

Screen snapshot of received power by the external dipole (around -56 dBm)

The transmitter output power is around -23 dBm, the received power by the external dipole is around -56 dBm. Therefore the path loss is around 33 dB, and the theoretic result from HFSS simulation of the coupling strength is around -29 dB at a coupling distance of 20 mm.

20

In-Vivo Tests of A CP Antenna

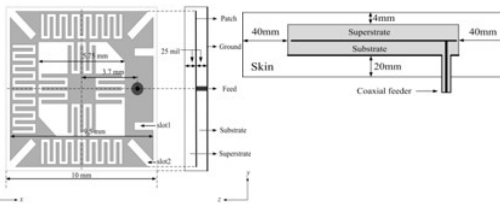

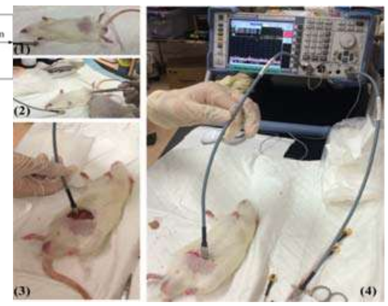

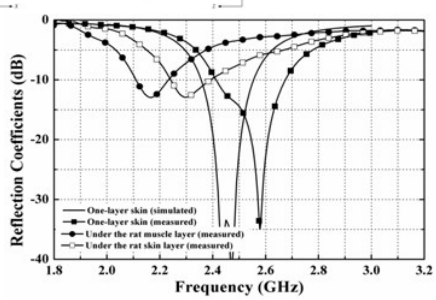

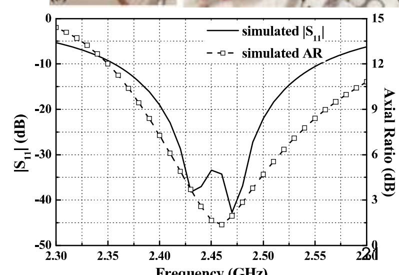

- C.R. Liu, Y.X. Guo, S.Q. Xiao, Capacitively Loaded Circularly Polarized Implantable Patch Antenna for ISM-Band Biomedical Applications, IEEE Transactions on Antennas and Propagation, vol. 62, no.5, pp. 2407-2417, May 2014.

21

Dual-band Capsule Antenna

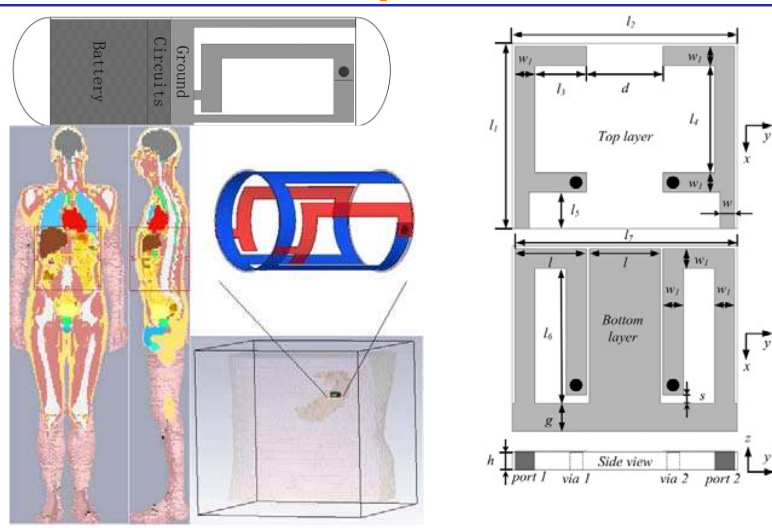

Z. Duan, Y.X. Guo, M. Je, and D.L. Kwong, Design and in vitro test of differentially fed dual-band implantable antenna operating at MICS and ISM bands, IEEE Transactions on Antennas and Propagation, vol. 62, no.5, pp. 2430-2439, May 2014.

22

Wireless Power and RF energy harvesting

- **Introduction:**
  - Need for Wireless Power and Data Telemetry
- **Wireless Power Delivery Schemes**
  - Near-field Inductive Power Transfer Links
  - Near-field Capacitive Power Transfer Links
  - Far-field Power Transfer Links
- **RF Energy Harvesting**

Wireless Power and RF energy harvesting

- Z.T. Liu, Z. Zhong, Y.X. Guo, Rapid design approach of optimal efficiency magnetic resonant wireless power transfer system, accepted by Electronics Letters.
- Z.T. Liu, Z. Zhong, Y.X. Guo, Enhanced Dual-band Ambient RF Energy Harvesting with Ultra-Wide Operating Power Range, IEEE Microwave and Wireless Components Letters, vol. 25, no.9, pp. 630-622, 2015
- R. Jegadeesan, S. Nag, K. Agarwal, N.V. Thakor, and Y.X. Guo, Enabling Wireless Powering and Telemetry for Peripheral Nerve Implants, IEEE Journal of Biomedical and Health Informatics, vol. 19, no.3, pp. 958-970, May 2015.
- C.R. Liu, Y.X. Guo, H.C. Sun, S.Q. Xiao, Design and Safety Considerations of an Implantable Rectenna for Far-Field Wireless Power Transfer, IEEE Transactions on Antennas and Propagation, vol. 62, no.11, pp. 5798-5806, Nov 2014.
- R. Jegadeesan, Y.X. Guo, Topology Selection and Efficiency Improvement of Inductive Power Links, IEEE Transactions on Antennas and Propagation, vol. 60, no. 10, pp. 4846-4854, Oct 2012.
- Z. Duan, Y.X. Guo, D.L. Kwong, Rectangular Coils Optimization for Wireless Power Transmission, Radio Science, vol. 47, no. RS012, pp. 1-10, June 2012.
- R. Jegadeesan, Y.X. Guo, M. Je, Overcoming coil misalignment using magnetic fields of induced currents in wireless power transmission, IEEE MTT-S IMS 2012.
- H. C. Sun, Z. Zhong, and Y.-X. Guo, “An adaptive reconfigurable rectifier for wireless power transmission,” Electronics Letters, vol. 49, no. 18, Aug 2013.
- H. C. Sun, Y.-X. Guo, M. He, and Z. Zhong, “A dual-band rectenna using broad-band Yagi antenna array for ambient RF power harvesting,” IEEE Antennas and Wireless Propagation Letters, vol. 12, pp. 918-921, 2013.
- H. C. Sun, Z. Zhong, and Y.-X. Guo, “An adaptive reconfigurable rectifier for wireless power transmission,” IEEE Wireless and Components Letters, vol. 23, no.9, pp. 492-494, Sept 2013.
- H. C. Sun, Y.-X. Guo, M. He, and Z. Zhong, “Design of a high-efficiency 2.45-GHz rectenna for low-input-power energy harvesting,” IEEE Antennas and Wireless Propagation Letters, vol. 11, pp. 929–932, 2012.

Related Patent Applications:
Y.X. Guo, Z. Zhong, H.C. Sun, Rectenna circuit elements, circuits, and techniques for efficiency wireless power transmission or ambient RF energy harvesting, filed for PCT on Feb 27, 2014, PCT international publication number WO 2014/133461 A1; US application number 14/767,125; Chinese Patent Application No. 201480011007.1

Need for Wireless Power Delivery

- Wireless power delivery is hassle-free and aesthetic
  - Power limitations exist
  - but sufficient for most implants
  - Extra implant-side coil and electronics
- Power Budget – Most permanent implants require

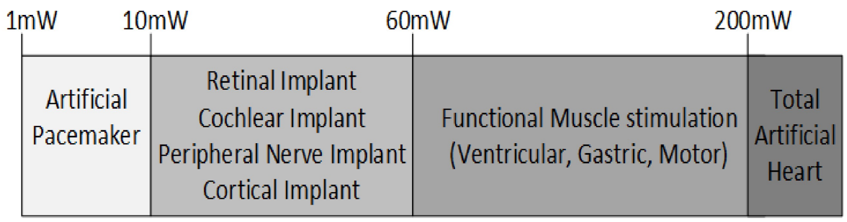

 25

Wireless Power Link for muscle stimulation

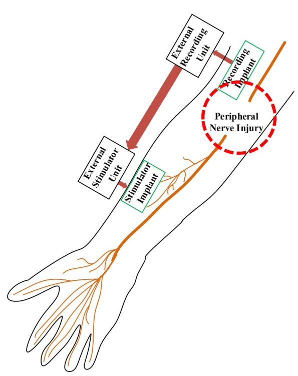

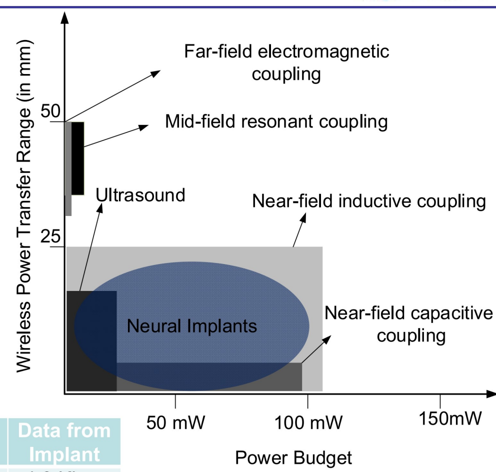

Implant type	Power Requirement	Data to Implant	Data from Implant
Stimulation	100 mW	4.8 Kbps	4.8 Kbps
Recording	35 mW	NA	1.3 Mbps

 26

R. Jegadeesan, S. Nag, K. Agarwal, N. V. Thakor and Y. X. Guo, "Enabling Wireless Powering and Telemetry for Peripheral Nerve Implants" *IEEE Journal of Biomedical and Health Informatics*, May 2015.

Inductive Wireless Power

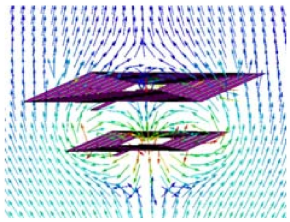

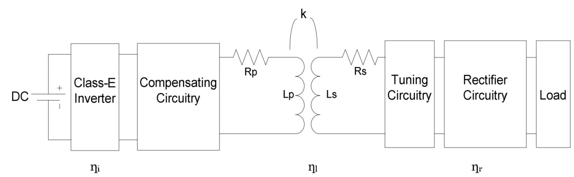

- **Inductive power transmission** is one important power transfer method for implants.
- **Efficient wireless power transfer** methods have a significant reduction of power loss in the implants, thereby eliminating **health hazards** due to the **heat produced**.
- The **challenges** for inductive links in biomedical implants lie in varying coupling coefficients due to the presence of air, skin, tissues and variation in separation and misalignment between the coupled coils.

 27

Four Possible Topologies

• The type of resonance(Series/parallel) in the secondary side and the type of compensation(Series/Parallel) in the primary side gives raise to four possibilities : SS , SP, PS and PP topologies.

• It would be insightful to derive the efficiency expressions for the power transferred to the load and identify which topology is better for a specific wireless link.

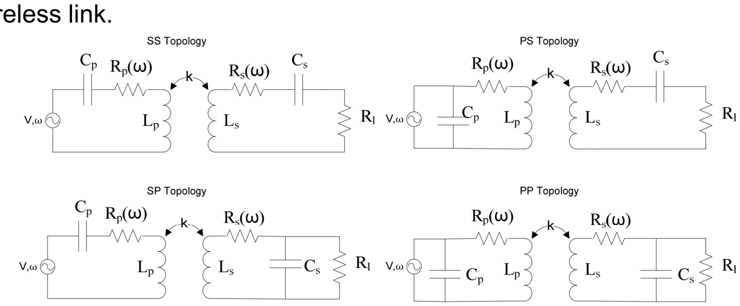

R. Jegadeesan, **Y.X. Guo**, Topology Selection and Efficiency Improvement of Inductive Power Links, IEEE Transactions on Antennas and Propagation, vol. 60, no. 10, pp. 4846-4854, Oct 2012.

 28

Efficiency Expressions

$$\eta_{ss/ps} = \frac{1}{1 + \frac{R_s(\omega)}{R_l} + \frac{R_p(\omega)}{k^2 L_p R_l}\left\{L_s + \left[\frac{\left(R_l + R_s(\omega)\right)^2}{L_s} - \frac{2}{C_s}\right]\frac{1}{\omega^2} + \left(\frac{1}{L_s C_s^2}\right)\frac{1}{\omega^4}\right\}}$$

$$\eta_{sp/pp} = \frac{1}{1 + \frac{R_s(\omega)}{R_l} + \omega^2 R_l R_s(\omega) C_s^2 + \frac{R_p(\omega)}{k^2 L_p L_s R_l}\left\{\left[\frac{(1-\omega^2 L_s C_s) R_l + R_s(\omega)}{\omega}\right]^2 + [L_s + R_l C_s R_s(\omega)]^2\right\}}$$

• It must be noted that the type of resonance at the secondary determines the efficiency of the wireless link, irrespective of the type of primary compensation used. Hence it would suffice if we compare the SS topology with the SP topology.

• The compensating capacitor in the primary side does not affect the efficiency of the wireless link, and hence serves as an independent parameter that can control the power transferred to the load without affecting the efficiency.

Maximizing Efficiency

- The efficiency expressions were maximized with respect to the secondary capacitance (Cs) in both the topologies and the maximum efficiency was found as

$$\eta_{ss/ps}^{max} = \frac{1}{1 + \frac{R_s(\omega)}{R_l} + \frac{R_p(\omega)\left(R_l + R_s(\omega)\right)^2}{k^2 L_p L_s \omega^2 R_l}}$$

$$\eta_{sp}^{max} = \frac{1}{1 + \frac{R_s(\omega)}{R_l} + \frac{R_l R_s(\omega)}{L_s^2 \omega^2} + \frac{R_p(\omega)}{k^2 L_p L_s R_l}\left\{\left[\frac{R_s(\omega)}{\omega}\right]^2 + \left[L_s + \frac{R_l R_s(\omega)}{L_s \omega^2}\right]^2\right\}}$$

- It is to be noted that in both the topologies the coupling coefficient enhances the efficiency and the series resistances degrades the efficiency.
- However the effect of the load resistance, primary and secondary inductance on the efficiencies are different for both the topologies.

Efficiency Verification

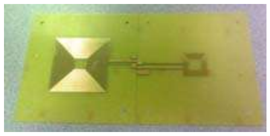

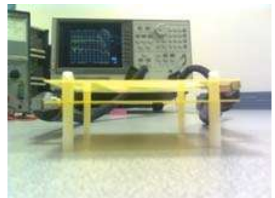

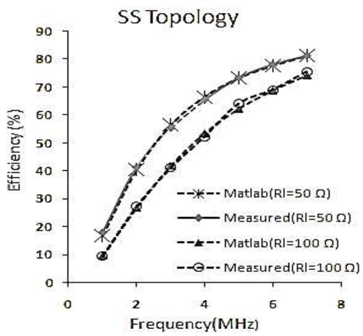

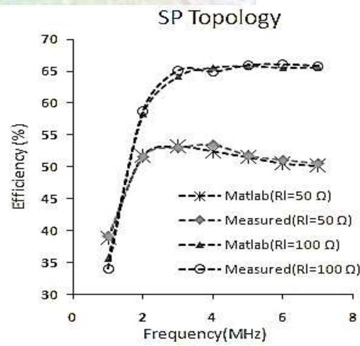

Cross Over Frequency (Fixed Load)

When the load is fixed and no matching networks are allowed, the topology that is more efficient needs to be selected based on the cross over frequency.

$$f_c = \frac{R_l}{2\pi L_s}\left(\sqrt{1-\frac{k^2 L_p R_s}{L_s R_p}}\right)$$

Measured values @ 3MHz:
Lp= 12.8 uH, Ls= 2.83 uh
Rp= 4.47 Ohm, Rs=2.67 Ohm
***k*= 0.173**

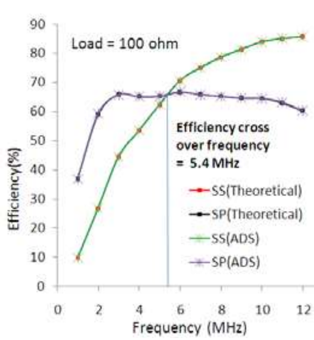

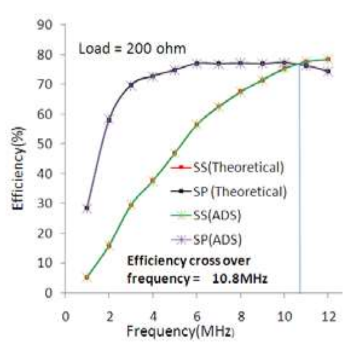

Optimal Load

If load is allowed to be chosen or matching network is allowed, the link can be matched to an optimized load which maximizes the power transfer efficiency.

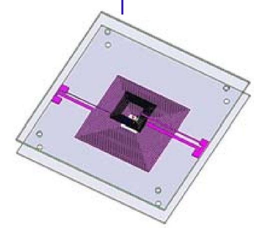

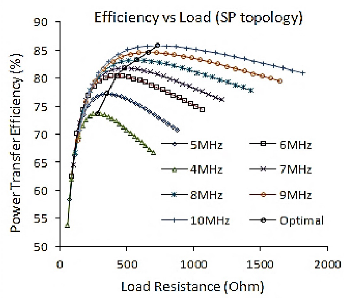

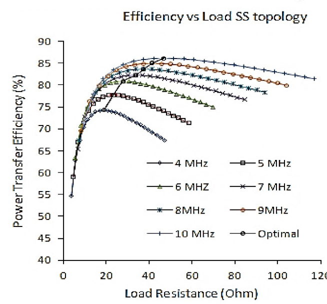

Application to Neural Implant

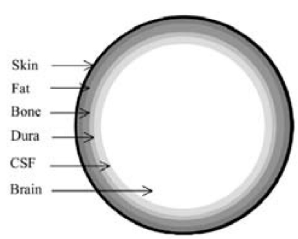

Schematic of the six-layered spherical head modeling a human head

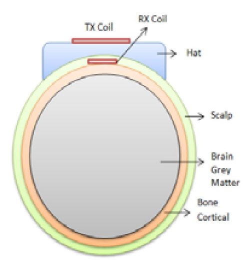

Coil Separation = 10.2mm

TABLE 2.2: Single-, Three- and Six-layered Spherical Head Models with an Outer Radius of 9 cm

BIOLOGICAL TISSUE	HOMOGENEOUS HEAD (cm)	THREE-LAYERED HEAD (cm)	SIX-LAYERED HEAD (cm)
Brain	$a_1 = 9.00$	$a_3 = 8.10$	$a_6 = 8.10$
CSF			$a_5 = 8.30$
Dura			$a_4 = 8.35$
Bone		$a_2 = 8.55$	$a_3 = 8.76$
Fat			$a_2 = 8.90$
Skin		$a_1 = 9.00$	$a_1 = 9.00$

Coil Dimension	Optimal Frequency	Trace Width	Efficiency
10mm	0.3GHz	1mm	49.51%
9mm	0.3GHz	0.9mm	47.1%
8mm	0.2GHz	0.8mm	35.1%
7mm	0.15GHz	0.8mm	28.08%
6mm	0.15GHz	0.8mm	27.19%

Coil Misalignment

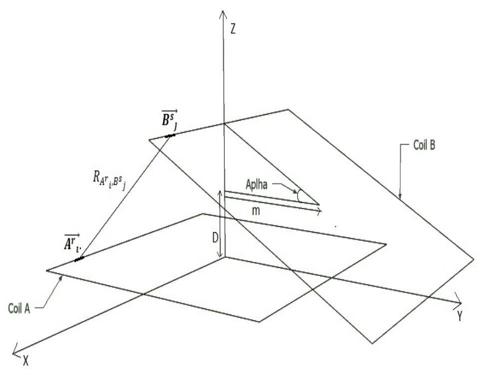

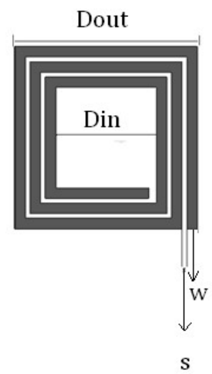

Square planar inductors A and B of turns N_A and N_B respectively separated by a distance D and have lateral(m) and angular(α) misalignment

Square Planar inductor, typical representation

 35

3-Coil Case

- IX coil is introduced to boost flux linkage.
- The efficiency improvement is quantified using our method by computing mutual inductance between the coils at various positions of the IX coil

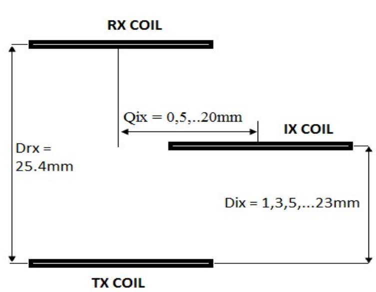

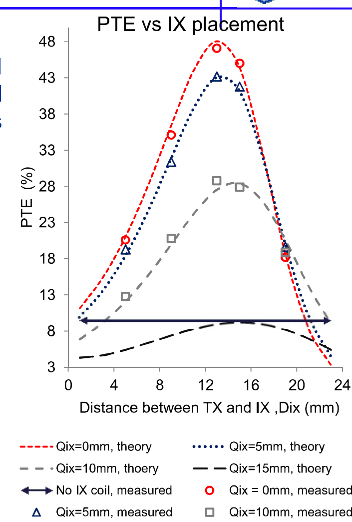

R. Jegadeesan, Y.X. Guo, M. Je, Overcoming coil misalignment using magnetic fields of induced currents in wireless power transmission, IEEE MTT-S IMS 2012. 36

Overcome coil misalignment

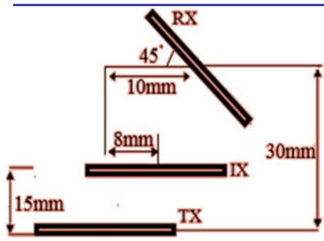

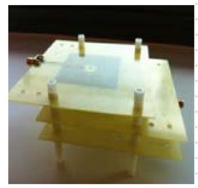

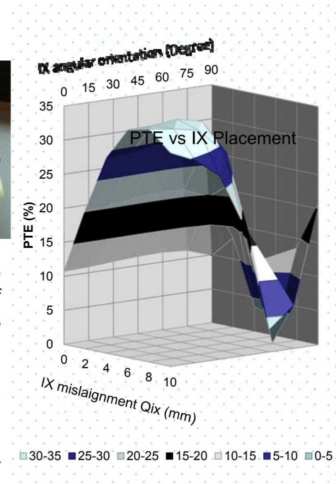

- For a receiving coil inclined at 45 degrees to the transmitting coil and having a lateral misalignment of 10mm, the optimal location of the intermediate coil is evaluated using our computation method for mutual inductance between misaligned coils .
- The IX coil is optimally positioned when placed at a distance of 15mm from the TX coil and has 8mm lateral misalignment with no angular orientation.
- The optimal Efficiency for the shown set up is 34%. The Power Transfer efficiency without flux linkage boosting is 2%.

 37

4-Coil Case - Retinal implant

Four coil topology for retinal implants improves the PTE and provides robustness to misalignment caused by rotation motion of eye ball.

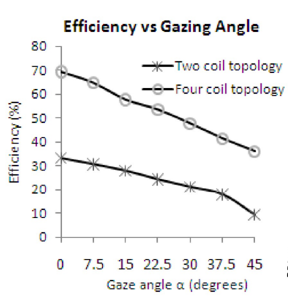

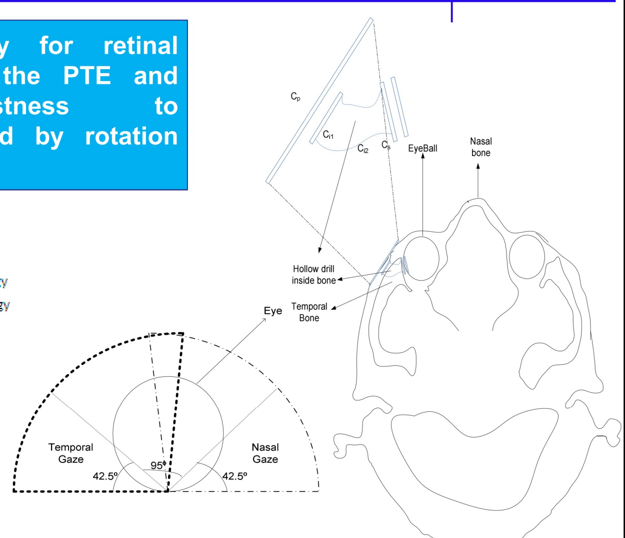

 38

Cadaver Head Experiment

• Optimized inductive power links
-secondary coil (8mm X 8mm, 13 turns)
-primary coil (40mm X 40mm, 20 turns)

Both anterior and lateral sub muscular method were tested.
-angular orientation of the coils (movement of the eyeballs)
- translation of the coils (possible motion artifacts).

Observations:

- 20-25% reduction in power delivered to the implant due to the introduction of bones .
- When the primary coil undergoes translation, there is a 10-15% reduction in power delivered to the implant.
- The power delivered to the implant reduces considerably as the inclination of the primary coil with respect to the secondary coil increases.
- The wireless power link was able to transfer a maximum power of 6mW with an input power of 37.5mW for a separation of 25mm.

39

Capacitive Wireless Power

NUS National University of Singapore

• Wireless power transfer for biomedical implants using capacitive coupling (electric near field coupling) provides an attractive alternative to the traditional inductive coupling method with the benefits of simple topology, fewer components on the implant side, better EMI performance and robustness to surrounding metallic elements.

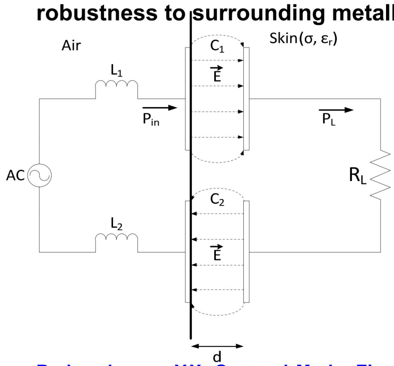

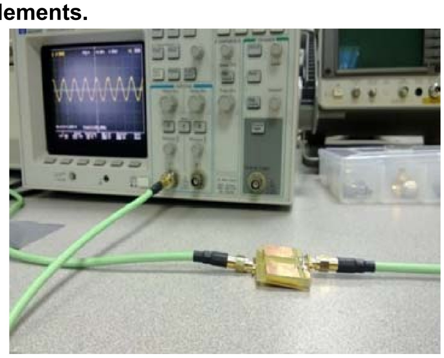

R. Jegadeesan, Y.X. Guo and M. Je, Electric Near-Field Coupling for Wireless Power Transfer in Biomedical Applications, IEEE MTT-S International Microwave Workshop Series on RF and Wireless Technology for Biomedical Healthcare Applications, Singapore, Dec 9-11, 2013.

40

In-Vivo Capacitive Power Transfer

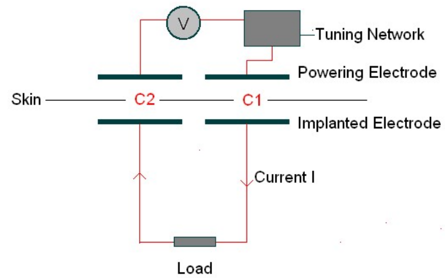

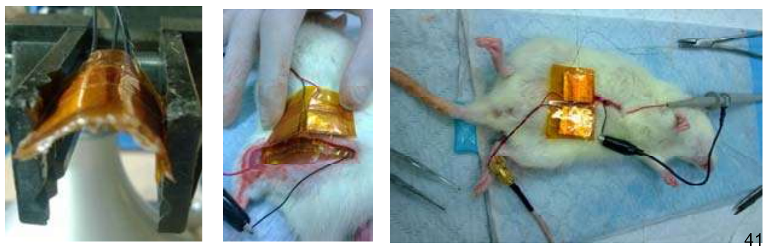

 41

In-Vivo Capacitive Power Transfer - Skin Thickness and Bending Effects

Link Parameter	Values		
	3mm skin	4mm skin	5mm skin
Separation between patches 'd'	4.6mm	5.6mm	6.6mm
Area of patches	380 mm^2	380 mm^2	380 mm^2
Load	50 ohm	50 ohm	50 ohm
Power transfer efficiency at 402 MHz (Measured)	68.3%	67.2%	67.0%
Power transfer efficiency[1-2] at 402 MHz (Computed)	72.85%	72.78%	72.63%
Average SAR (10mw at receiver)	7.9E-2 W/Kg	8.4E-2 W/Kg	1.2E-1 W/Kg

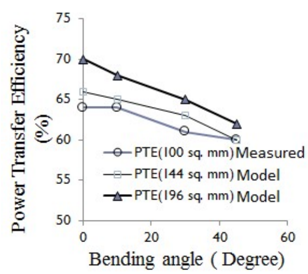

 42

Far-Field Wireless Power

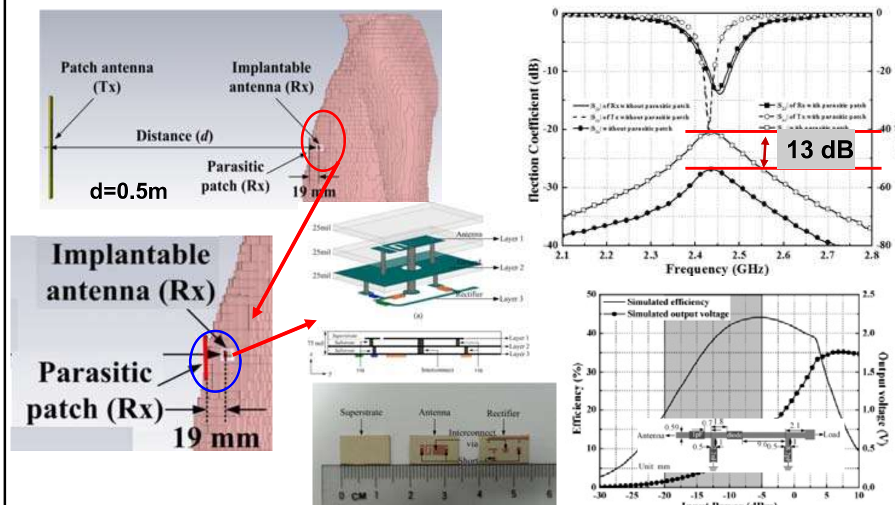

C.R. Liu, Y.X. Guo, H.C. Sun, S.Q. Xiao, Design and Safety Considerations of an Implantable Rectenna for Far-Field Wireless Power Transfer, IEEE Transactions on Antennas and Propagation, vol. 62, no.11, pp. 5798-5806, Nov 2014.

43

Wireless Energy Harvesting

44

Rectenna Design for Wireless Power Transmission

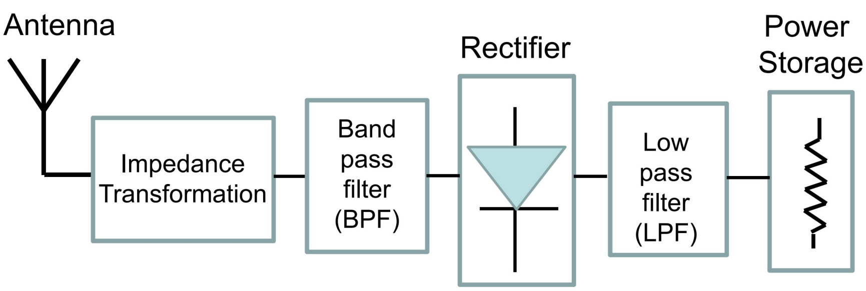

A rectenna is a rectifying antenna, a special type of antenna that is used to directly convert microwave energy into DC electricity.

A simplest rectenna element consists of an antenna (or antenna array) with a Schottky diode placed across the antenna elements. The diode rectifies the RF current induced in the antenna by the microwaves, to produce DC power. Schottky diodes are used because they have the lowest voltage drop and highest speed and therefore waste the least amount of power due to conduction and switching. Good rectennas consist of impedance transformation, band pass filter and low pass filter to improve its RF-DC conversion efficiency .

Adaptive Rectifier Design

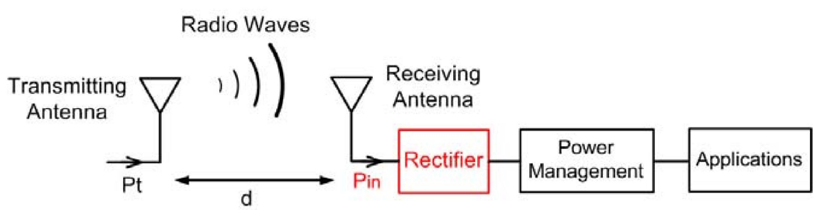

Fig. 1. Overview of the wireless power transmission system.

- Requirement for Rectifier Design

Pin changes if
- Pt varies
- d changes
- Receiving antenna is on mobile devices.

Requirement for rectifier → High efficiency over wide input power range.

Adaptive Rectifier Design

NUS National University of Singapore

➢ Diode Selection for Rectifier

•Threshold Voltage (Vth) —determines→ rectifier's efficiency at low input power.

Low Vth is preferred for low-input-power applications.

•Breakdown Voltage (Vbr) —determines→ rectifier's efficiency at high input power.

High Vbr is preferred for high-input-power applications.

➢ Limitation of Normal Rectifier

Low Vth and high Vbr cannot be obtained at the same time.

↓

High efficiency can only be achieved in a narrow input power range.

Adaptive Rectifier Design

NUS National University of Singapore

➢ Limitation Illustration

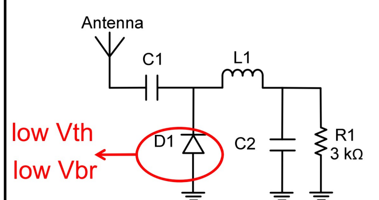

(a) Single shunt-mounted diode.

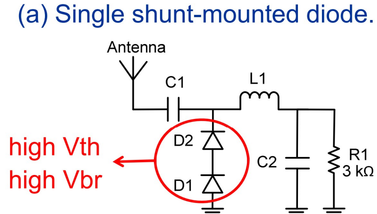

(b) Two shunt-mounted diodes.

Efficiencies versus input power.

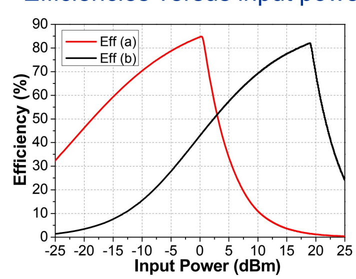

- Rectifier (a) is only suitable for low-input-power applications.
- Rectifier (b) is only suitable for high-input-power applications.

Operation Mechanism of Proposed Rectifier

Depletion-mode field-effect transistor (FET) as a switch.

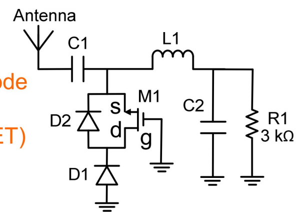

(c) Two diodes with one FET as a switch.

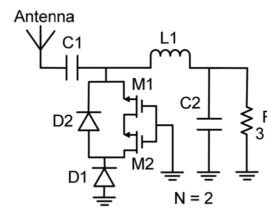

(d) Two diodes with two FETs as a switch.

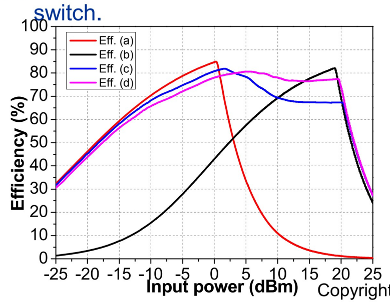

- Rectifier (c): small Vth and large Vbr can be achieved for the combination of D1 and D2.
  High efficiency -18 dBm to 22 dBm.
- Rectifier (d): two FETs to enhance efficiency from 5 dBm to 20 dBm.

 49

Adaptive Rectifier Design

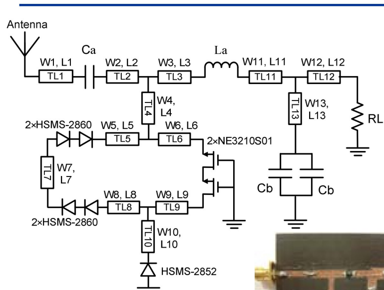

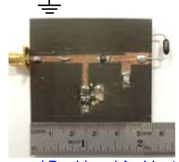

Simulated efficiencies versus input power

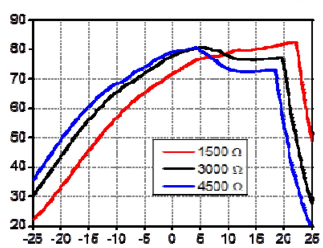

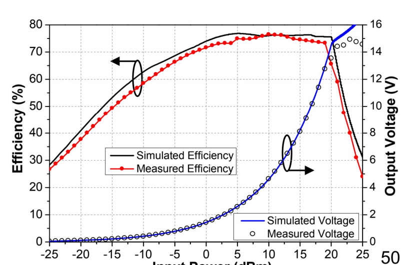

- Z.T. Liu, Z. Zhong, Y.X. Guo, Enhanced Dual-band Ambient RF Energy Harvesting with Ultra-Wide Operating Power Range, IEEE Microwave and Wireless Components Letters, vol. 25, no.9, pp. 630-622, 2015
- H. C. Sun, Z. Zhong, and Y.X. Guo, "An adaptive reconfigurable rectifier for wireless power transmission," Electronics Letters, vol. 49, no. 18, Aug 2013.
- H. C. Sun, Z. Zhong, and Y.X. Guo, "An adaptive reconfigurable rectifier for wireless power transmission," IEEE Wireless and Components Letters, vol. 23, no.9, pp. 492-494, Sept 2013.

 50

Wideband Patch Antennas

- Y.X. Guo, M.Y.W. Chia, Z.N. Chen, and K.M. Luk, Wideband L-probe fed circular patch antenna for conical-pattern radiation, IEEE Trans Antennas and Propagation, vol. 52, No.4, pp. 1115-1116, April 2004.
- Y.X. Guo, K.M. Luk, and K.F. Lee, Broadband dual polarization patch element for cellular-phone base stations, IEEE Trans. Antennas and Propagation, vol. 50, no.2, pp. 251-253, Feb 2002.
- Y.X. Guo, C.L. Mak, K.M. Luk, and K.F. Lee, Analysis and design of L-probe proximity fed patch antenna, IEEE Trans. Antennas and Propagation, vol. 49, no.2, pp.145-149, Feb. 2001.
- Y.X. Guo, K.M. Luk, and K.F. Lee, L-probe proximity-fed annular ring microstrip antennas, IEEE Trans. Antennas and Propagation, vol.49, no.1, pp.19-21, Jan. 2001.
- Y.X. Guo, K.M. Luk, and K.F. Lee, L-probe proximity-fed short-circuited patch antennas, IEE Electronics Letters, vol. 35, no. 24, pp.2069-2070, Nov 1999.
- Y.X. Guo, K.M. Luk, K.F. Lee, and Y.L. Chow, Double U-slot rectangular patch antenna, IEE Electronics Letters, vol. 34, no. 19, pp.1805-1806, Sept 1998.
- K.M. Luk, Y.X. Guo, K.F. Lee, and Y.L. Chow, L-probe proximity fed U-slot patch antenna, IEE Electronics Letters, vol. 34, no. 19, pp.1806-1807, Sept 1998.

 51

Wideband Antenna Design

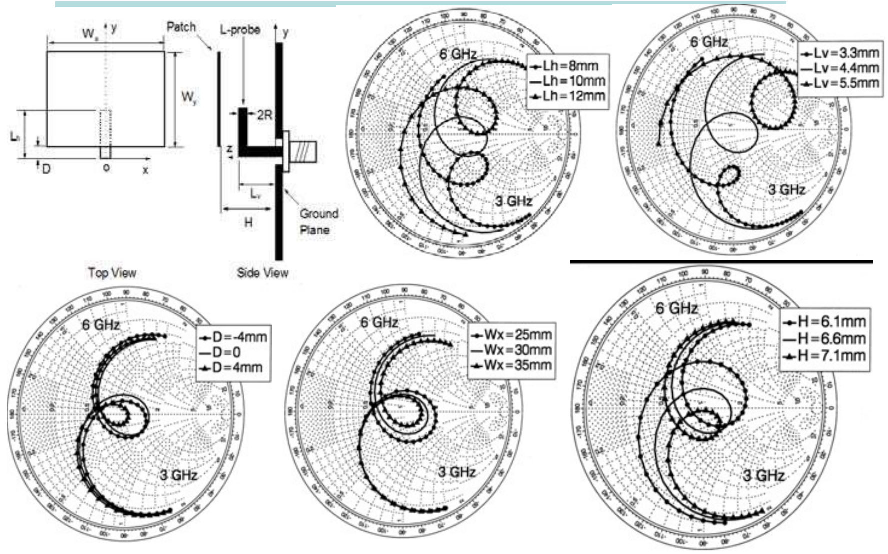

Y.X. Guo, C.L. Mak, K.M. Luk, and K.F. Lee, Analysis and design of L-probe proximity fed patch antenna, IEEE Trans. Antennas and Propagation, vol. 49, no.2, pp.145-149, Feb. 2001.

52

Wideband Annular Ring Patch Antenna

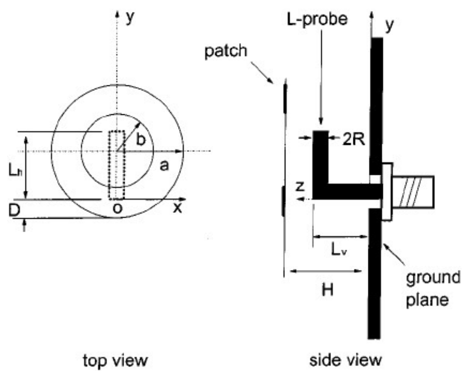

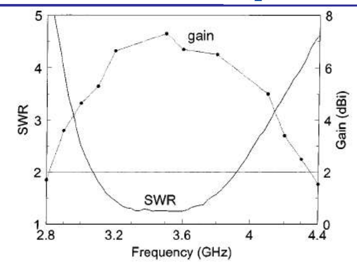

SWR and gain for the TM_{11} mode.

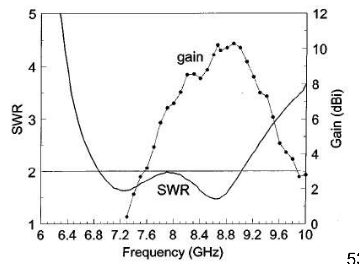

SWR and gain for the TM_{12} mode.

Y.X. Guo, K.M. Luk, and K.F. Lee, L-probe proximity-fed annular ring microstrip antennas, IEEE Trans. Antennas and Propagation, vol.49, no.1, pp.19-21, Jan. 2001.

Wideband Dual-Polarization Patch Antenna

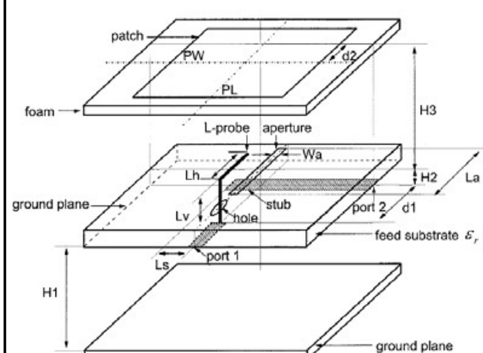

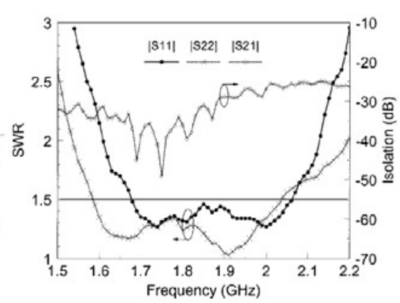

Y.X. Guo, K.M. Luk, and K.F. Lee, Broadband dual polarization patch element for cellular-phone base stations, IEEE Trans. Antennas and Propagation, vol. 50, no.2, pp. 251-253, Feb 2002.

Wideband Patch Antenna with Conical Radiation Pattern

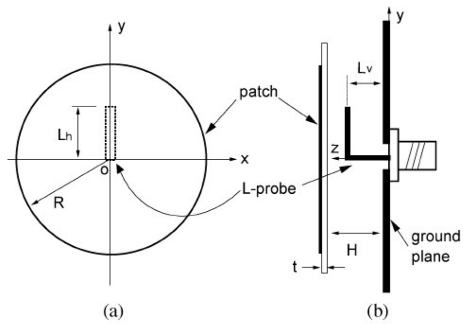

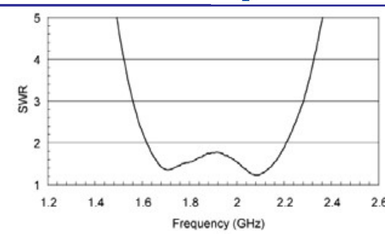

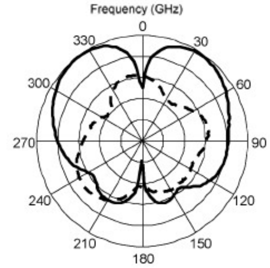

yz plane

Y.X. Guo, M.Y.W. Chia, Z.N. Chen, and K.M. Luk, Wideband L-probe fed circular patch antenna for conical-pattern radiation, IEEE Trans Antennas and Propagation, vol. 52, No.4, pp. 1115-1116, April 2004.

Wideband Patch Antennas with Broadband Feeding Networks

- Z.Y. Zhang, **Y.X. Guo**, L.C. Ong, and M.Y.W. Chia, "A new wideband planar balun on a single-layer PCB", IEEE Microwave and Wireless Components Letters, vol. 15, no.6, pp. 416-418, 2005.
- **Y. X. Guo**, Z. Y. Zhang, and L. C. Ong, "Improved wideband Schiffman phase shifter," *IEEE Trans. Microw. Theory Tech.* , vol. 54, no. 3, pp. 1196-1200, Mar. 2006.
- L. Bian, **Y. X. Guo**, L. C. Ong, and X. Q. Shi, "Wideband Circularly Polarized Patch Antenna,"*IEEE Trans. Antennas Propag.* , vol. 54, no. 9, pp. 2682-2686, Sep. 2006.
- **Y.X. Guo**, K.W. Khoo, L.C. Ong, and K.M. Luk, Wideband Low Cross-Polarization Patch Antenna Using A Broadband Balun Feed Network, Radio Science, vol. 42, RS5008, doi:10.1029/2006RS003595, Oct 2007.
- **Y.X. Guo**, K.W. Khoo, L.C. Ong, Wideband dual-polarized planar antenna with broadband baluns, IEEE Transaction on Antennas and Propagation, vol. 55, no.1, pp. 78-83, Jan 2007.
- **Y.X. Guo**, K.W. Khoo, L.C. Ong, Wideband Circularly-Polarized planar antenna with broadband baluns, IEEE Transaction on Antennas and Propagation, vol. 56, no.2, pp. 319-326, Feb 2008.
- **Y.X. Guo,** L. Bian, X.Q. Shi, Wideband Circularly Polarized Annular-Ring Microstrip Antenna, IEEE Transactions on Antennas and Propagation, vol. 57, no. 8, pp. 2474-2477.

Feed Network Comparison

Conventional Narrowband Balun

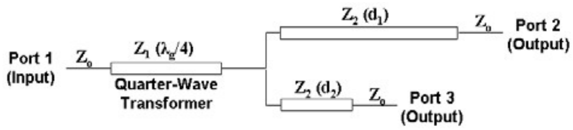

- Narrowband 180° phase shifting capabilities

Proposed Broadband Balun

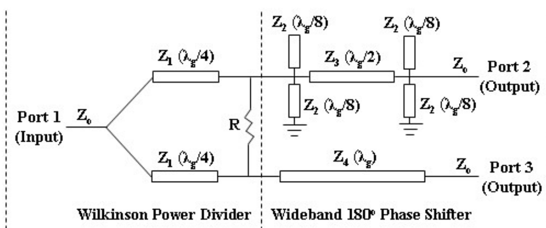

- Broadband 180° phase shifting capabilities

 57

Feed Network Comparison: Amplitude/Return Loss

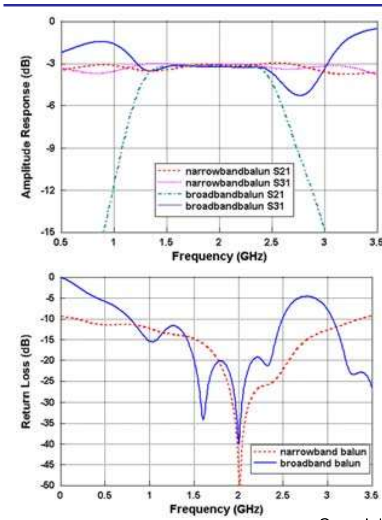

Conventional Narrowband Balun

- Balanced outputs ($S_{31} = S_{21} = -3$ dB) over a very wide band
- Wide impedance bandwidth ($S_{11} < -10$ dB) of 159%

Proposed Broadband Balun

- Balanced outputs ($S_{31} = S_{21} = -3$ dB) over a wide band of 60.5%
- Relatively narrower but still wide impedance bandwidth ($S_{11} < -10$ dB) of 70%

 58

Feed Network Comparison: Phase

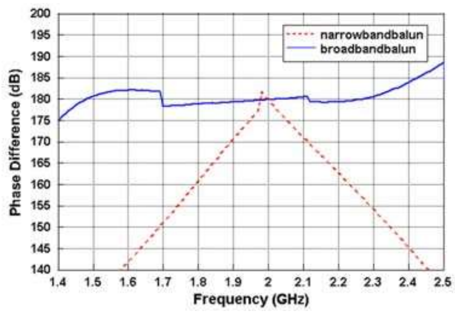

Conventional Narrowband Balun

- 180° (±5°) output ports phase difference only at frequency points near operating frequency

Proposed Broadband Balun

- 180° (±5°) output ports phase difference across a wide band of 38.4% from 1.6 to 2.4 GHz

Proposed Wideband Feed Network

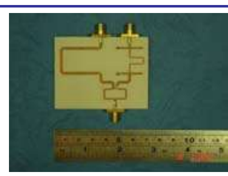

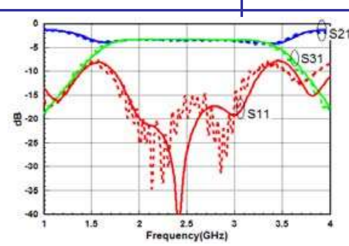

- 180° (±5°) output ports phase difference across a wide band of 38.4% from 1.6 to 2.4 GHz

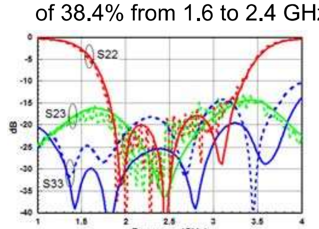

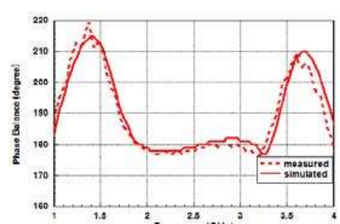

Z.Y. Zhang, **Y.X. Guo**, L.C. Ong, and M.Y.W. Chia, "A new wideband planar balun on a single-layer PCB", IEEE Microwave and Wireless Components Letters, vol. 15, no.6, pp. 416-418, 2005.

Broadband Low X-Pol Antennas

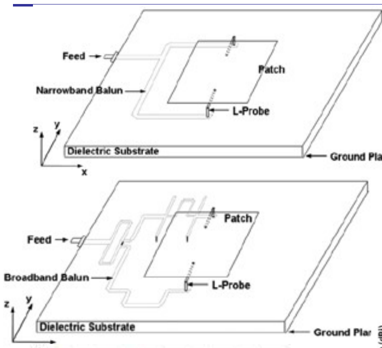

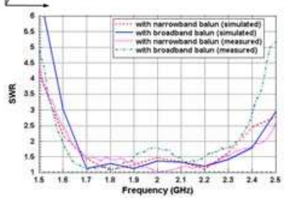

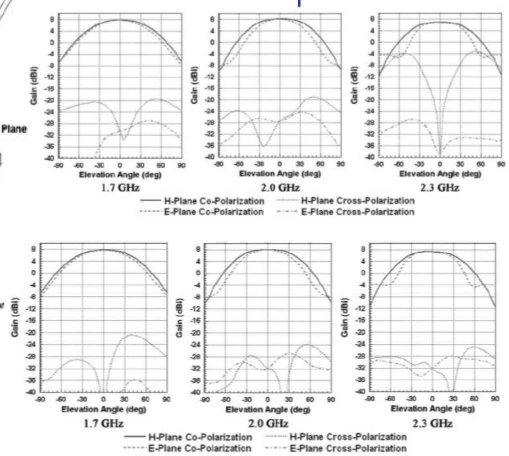

Y.X. Guo, K.W. Khoo, L.C. Ong, and K.M. Luk, Wideband Low Cross-Polarization Patch Antenna Using A Broadband Balun Feed Network, Radio Science, vol. 42, RS5008, doi:10.1029/2006RS003595, Oct 2007.

 61

Wideband Patch Antenna: Dual-Polarization

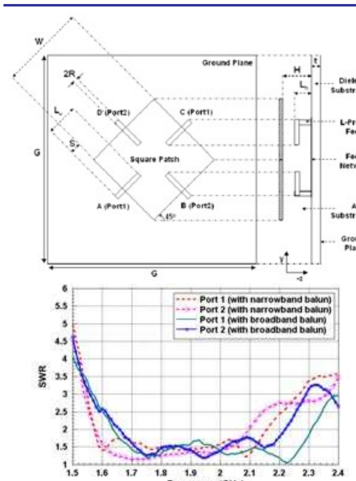

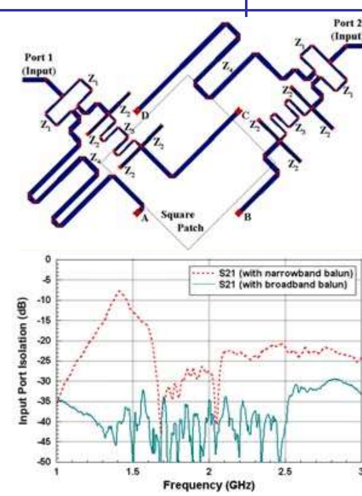

Y.X. Guo, K.W. Khoo, L.C. Ong, Wideband dual-polarized planar antenna with broadband baluns, IEEE Transaction on Antennas and Propagation, vol. 55, no.1, pp. 78-83, Jan 2007

62

Prior-Art Wideband CP Antennas

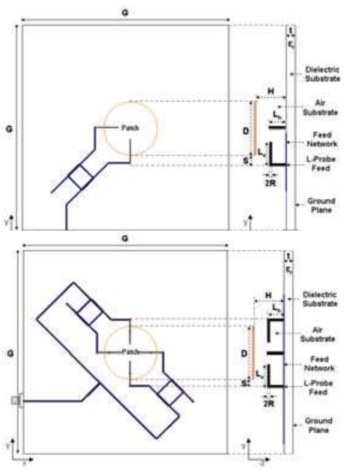

- Wide impedance (SWR <2) and 3-dB axial ratio bandwidths of 42% and 27.23%, respectively
- Wide impedance (SWR < 2) and 3-dB axial-ratio bandwidths of 45% and 45%, respectively

W. K. Lo, C. H. Chan, and K. M. Luk, "Bandwidth enhancement of circularly polarized microstrip patch antenna using multiple L-shaped probe feeds," *Microw. Opt. Technol. Lett.*, vol. 42, no. 4, pp. 263-265, Aug. 2004.

90^o Wideband Feed Network

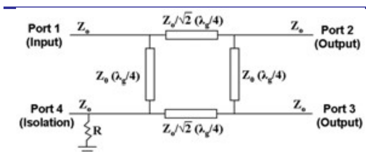

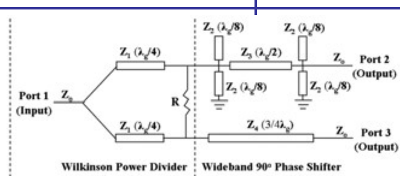

Provides impedance matching, balanced power splitting and 90^o ($\pm$5^o) phase shifting across a narrow bandwidth of 14%

Provides impedance matching, balanced power splitting and 90^o ($\pm$3^o) phase shifting across a wide bandwidth of 75%

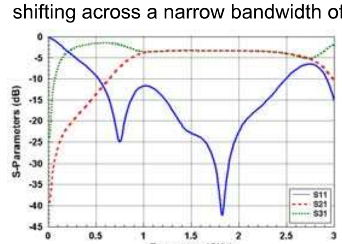

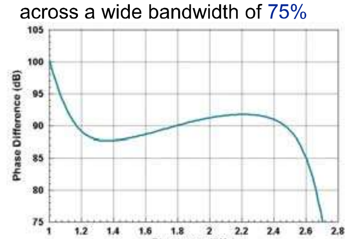

L. Bian, **Y. X. Guo**, L. C. Ong, and X. Q. Shi, "Wideband Circularly Polarized Patch Antenna," *IEEE Trans. Antennas Propag.* , vol. 54, no. 9, pp. 2682-2686, Sep. 2006.

Wideband CP Patch Antenna:

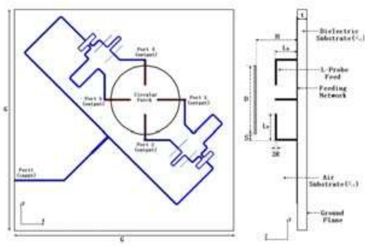

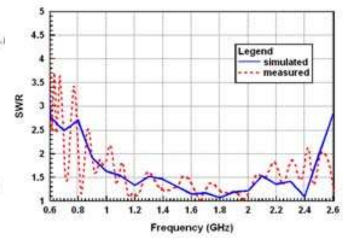

- Impedance bandwidth (SWR < 2) of 79.4%

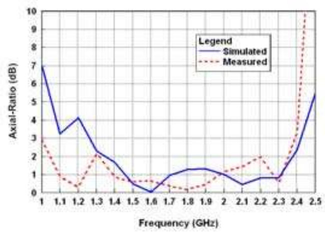

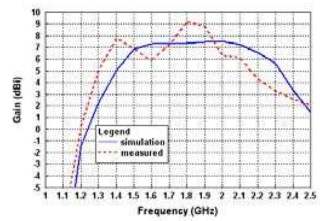

- 3-dB axial-ratio bandwidth of 82%
- Gain bandwidth (Gain > 3 dBic) of 59.3%

Wideband 90° Schiffman Phase shifter

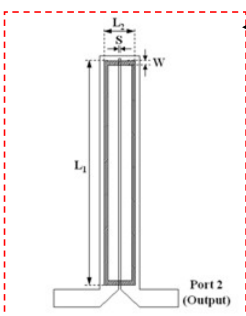

C-Section Coupled Lines

L_1 = 24.4 mm, L_2 = 4 mm, S = 0.3 mm, W = 0.5 mm

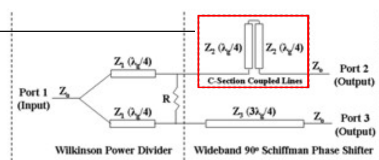

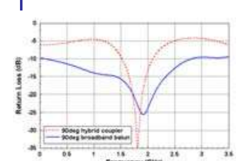

- Rectangular slot on the ground plane layer allows for even-mode capacitance to decrease faster than odd-mode capacitance
- Patterned ground plane approach incurs minimal insertion losses

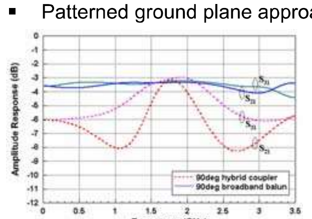

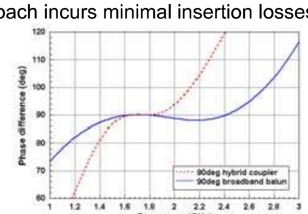

Y. X. Guo, Z. Y. Zhang, and L. C. Ong, "Improved wideband Schiffman phase shifter," *IEEE Trans. Microw. Theory Tech.*, vol. 54, no. 3, pp. 1196-1200, Mar. 2006.

Wideband CP Patch Antenna:

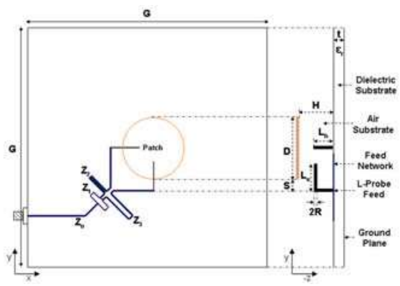

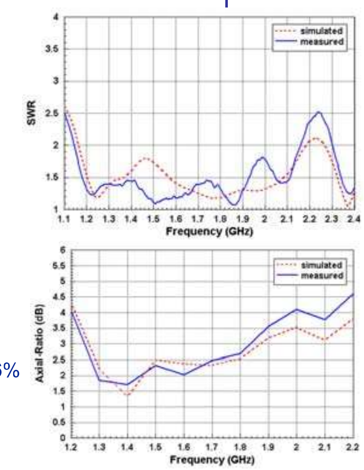

- Measured impedance bandwidth of 61.03%
- Measured 3-dB axial ratio bandwidth of 37.66%

Y.X. Guo, K.W. Khoo, L.C. Ong, Wideband Circularly-Polarized planar antenna with broadband baluns, IEEE Transaction on Antennas and Propagation, vol. 56, no.2, pp. 319-326, Feb 2008

Small Wideband and Multiband Antennas

- **Y.X. Guo**, K.M. Luk, K.F. Lee, and R. Chair, A quarter-wave U-shaped patch antenna with two unequal arms for wideband and dual-frequency operation, IEEE Trans. Antennas and Propagation, vol.50, no.8, pp.1082-1087, Aug 2002.
- **Y.X. Guo**, M.Y.W. Chia, and Z.N. Chen, "Miniature built-in quad-band antenna for mobile handsets," IEEE Antennas and Wireless Propagation Letters, vol.2, pp. 30-32, 2003.
- **Y.X. Guo**, M.Y.W. Chia, and Z.N. Chen, "Miniature built-in multiband antenna for mobile handsets," IEEE Trans AP, vol. 52, pp. 1936-1944, Aug 2004.
- Y.X. Guo, H.S. Tan, "New compact six-band internal antenna" IEEE Antennas and Wireless Propagation Letters, vol.3, pp. 295-297, 2004.
- I. Ang, **Y.X. Guo**, and M.Y.W. Chia, "Compact internal quad-band antenna for mobile phones," Microwave & Optical Technology Letters, vol. 38, no.3, pp. 217–233, August 5 2003.
- **Y.X. Guo**, I. Ang, and M.Y.W. Chia, "Compact internal multi-band antennas for mobile phones" IEEE Antennas and Wireless Propagation Letters, vol.2, pp. 143-146, 2003.

1. Small Dual-Band Antennas using Shorted Unequal-Arm U-Slot

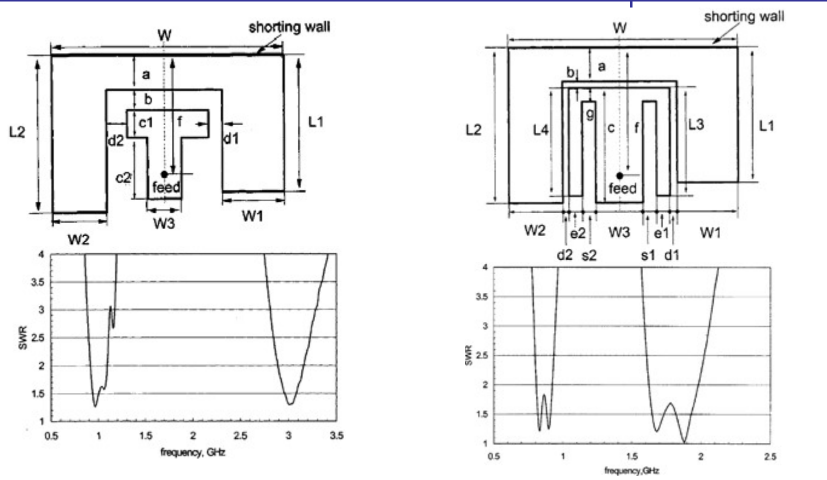

Y.X. Guo, K.M. Luk, K.F. Lee, and R. Chair, A quarter-wave U-shaped patch antenna with two unequal arms for wideband and dual-frequency operation, IEEE Trans. Antennas and Propagation, vol.50, no.8, pp.1082-1087, Aug 2002.

2. Quad-Band Internal Antennas

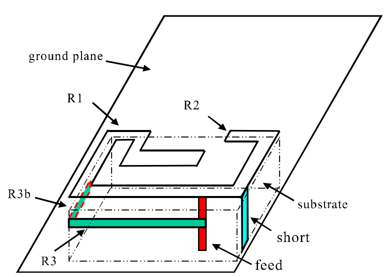

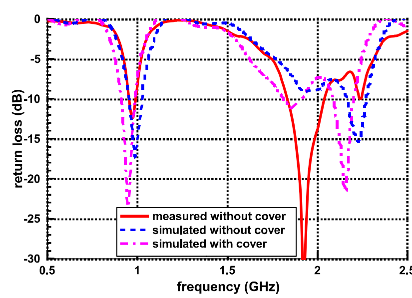

1. **Y.X. Guo**, M.Y.W. Chia, and Z.N. Chen, "Miniature built-in quad-band antenna for mobile handsets," IEEE Antennas and Wireless Propagation Letters, vol.2, pp. 30-32, 2003
2. **Y.X. Guo**, M.Y.W. Chia, and Z.N. Chen, "Miniature built-in multiband antenna for mobile handsets," IEEE Trans AP, vol. 52, pp. 1936-1944, Aug 2004
3. **Y.X. Guo**, M.Y.W. Chia, and Z.N. Chen, Miniature built-in multiple frequency band antenna, US Patent 6734825, granted in May 2004

3. Quad-Band Internal Antennas

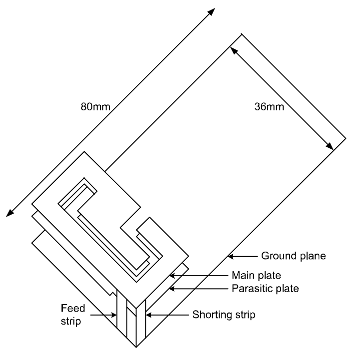

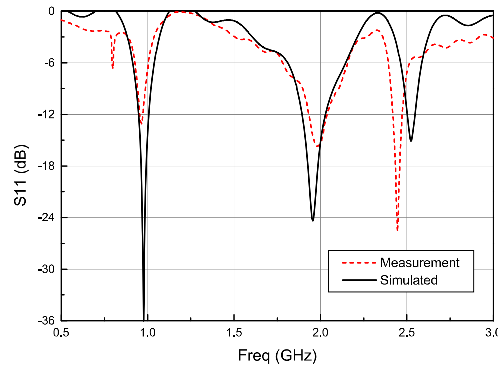

I. Ang, **Y.X. Guo**, and M.Y.W. Chia, "Compact internal quad-band antenna for mobile phones," Microwave & Optical Technology Letters, vol. 38, no.3, pp. 217–233, August 5 2003.

4. Quad-Band Internal Antennas

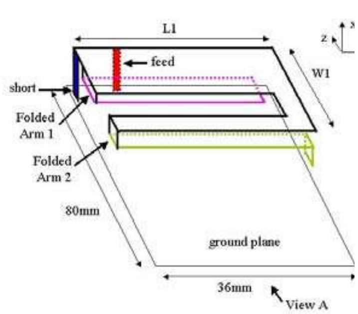

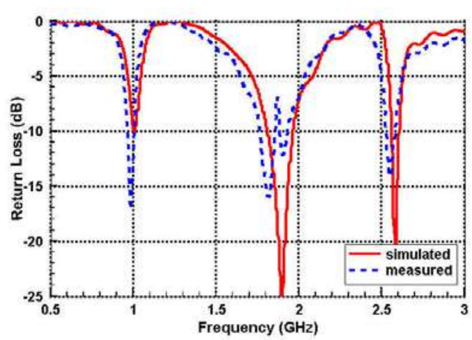

Y.X. Guo, I. Ang, and M.Y.W. Chia, "Compact internal multi-band antennas for mobile phones" IEEE Antennas and Wireless Propagation Letters, vol.2, pp. 143-146, 2003

Wideband Millimeter-Wave In-Package /On-Chip Antennas

NUS National University of Singapore

1. K. Kang, F. Lin, D. Pham, J. Brinkhoff, C.H. Heng, Y.X. Guo, X.J. Yuan, A 42-mW 60-GHz OOK Receiver with an On-chip Antenna in 90nm CMOS, IEEE Journal of Solid-State Circuits (JSSC), Vol. 45, No. 9, pp. 1720-1731, Sept 2010.
2. M.F. Karim, Y.X. Guo, M. Sun, J. Brinkhoff, L.C. Ong, K. Kang, F. Lin, Integration of SiP Based 60GHz 4*4 Antenna Array with CMOS OOK Transmitter and LNA, IEEE Transactions on Microwave Theory and Technique, vol. 59, no.7, 2011, pp. 1869-1878
3. M. Sun, Y.Q. Zhang, Y.X. Guo, K. Faeyz, L.C. Ong, M.S. Leong, Integration of Circular Polarized Array and LNA in LTCC as a 60-GHz Active Receiving Antenna, IEEE Transactions on Antennas and Propagation, vol. 59, no. 8, pp. 3083-3089, Aug 2011.
4. C.R. Liu, Y.X. Guo, X.Y. Bao, S.Q. Xiao, 60-GHz LTCC Integrated Circularly Polarized Helical Antenna Array, IEEE Transactions on Antennas and Propagation, vol. 60, no.3, pp. 1329-1335, Mar 2012.
5. X.Y. Bao, Y.X. Guo, Y.Z. Xiong, 60-GHz AMC-Based Circularly Polarized On-Chip Antenna Using Standard 0.18-μm CMOS Technology, IEEE Transactions on Antennas and Propagation, vol. 60, no.5, pp. 2234-2241, May 2012.
6. H Chu , Y.X. Guo, et al, 135-GHz Micromachined On-chip Antenna and Antenna Array, IEEE Transactions on Antennas and Propagation, vol. 60, no. 10, pp. 4582-4588, Oct 2012.
7. H. Chu, Y.X. Guo, Z.L. Wang, 60-GHz LTCC Wideband Vertical Off-Center Dipole Antenna and Arrays, IEEE Transactions on Antennas and Propagation, vol. 61, no.1, pp. 153-161, Jan 2013.
8. H.C. Sun, Y.X. Guo, Z.L. Wang, 60-GHz Circularly Polarized U-Slot Patch Antenna Array on LTCC, IEEE Transactions on Antennas and Propagation, vol. 61, no.1, pp. 430-435, Jan 2013.
9. L. Wang, Y.X. Guo, W.X. Sheng, Wideband High-Gain 60-GHz LTCC L-Probe Patch Antenna Array with a Soft Surface, IEEE Transactions on Antennas and Propagation, vol. 61, no.4, pt1, pp. 1802-1809, Apr 2013.
10. Y.J. Cheng, X.Y. Bao, Y.X. Guo, 60-GHz LTCC Miniaturized Substrate Integrated Multibeam Array Antenna with Multiple Polarizations, IEEE Transactions on Antennas and Propagation. vol. 61, no.12, pp. 5958-5967, Dec 2013
11. Y.J. Cheng, Y.X. Guo, X.Y. Bao, K.B. Ng, Millimeter-Wave Low Temperature Co-Fired Ceramic Leaky-Wave Antenna and Array Based on the Substrate Integrated Image Guide Technology, IEEE Transactions on Antennas and Propagation, vol. 62, pp. 669-676, Feb 2014.
12. Y.J. Cheng, Y.X. Guo, Z.G. Liu, W-Band Large-Scale High-Gain Planar Integrated Antenna Array, IEEE Transactions on Antennas and Propagation, vol. 62, pp. 3370-3373, June 2014

Antennas in Package

NUS National University of Singapore

On-Package Antenna solutions realize an antenna (or antennas) with highly-integrated radio die (or dies) into a standard surface mounted device symbolizing an innovative and important development in wireless frontier in recent years.

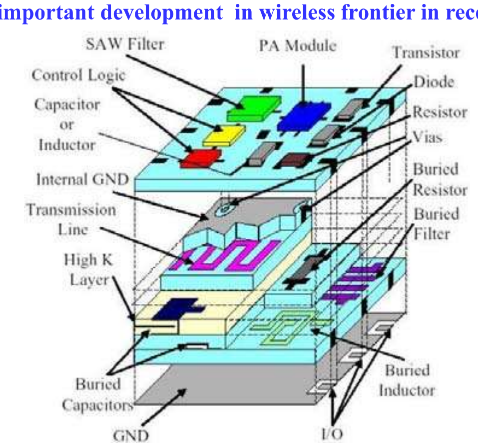

Millimeter-wave and Sub-THz Radios

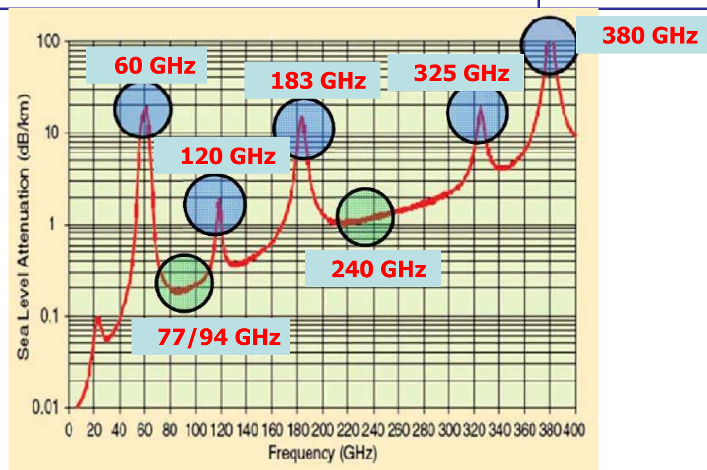

Source: T.S. Rappaport, et al, "State of the art in 60-GHz Integrated Circuits and Systems for Wireless Communications, " Proceedings of IEEE, Aug 2011.

 75

Why is Operation at 60 GHz Interesting

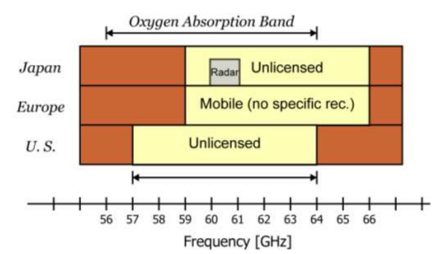

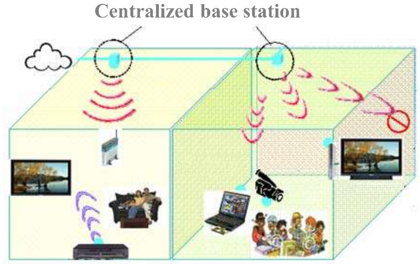

- License-free deployment
- Multi-gigabit operation
- Oxygen attenuates 60 GHz signals by 12-16 dB/km
- Immunity to interference
- Security from signal interception

- wireless replacement of cables

Wireless Personal Area Networks

- high definition video streaming

Wireless High-Definition Multimedia Interface (HDMI)

The intended range: 10 meters or less

 76

Applications of 60-GHz Radios

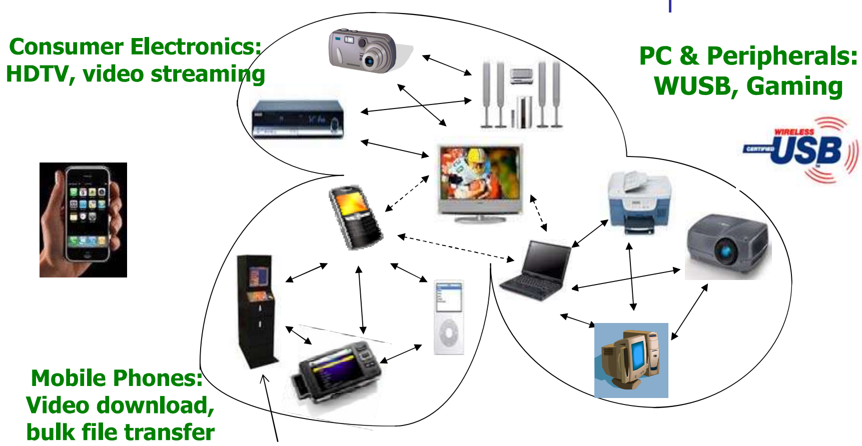

Wire-bonding Study at 60 GHz

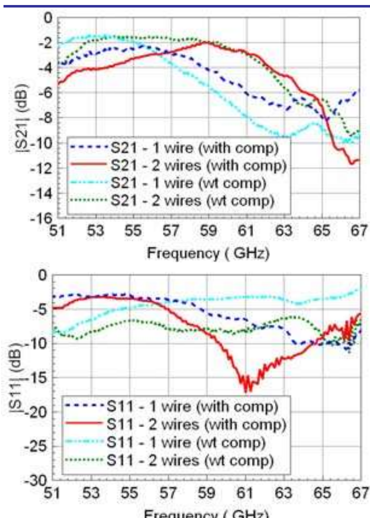

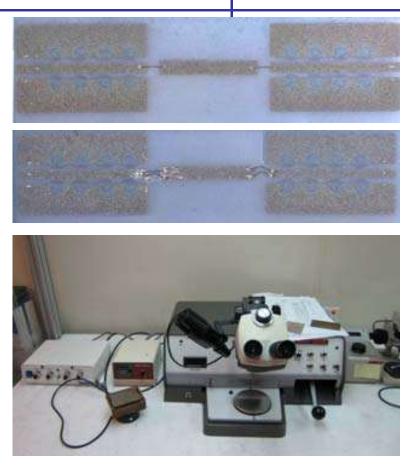

WEST® BONDER
Manual DIE/WIRE Bonder

Why CP Antennas

• The commonly used linearly-polarized (LP) antenna necessitates rotating the transmitting and receiving antenna properly for polarization matching, particularly in the case of the line-of-sight (LOS) radio links.

• Using the CP antenna this problem can be mitigated while also allowing for reduction in interference from multi-path reflections.

 79

Single CP Elements

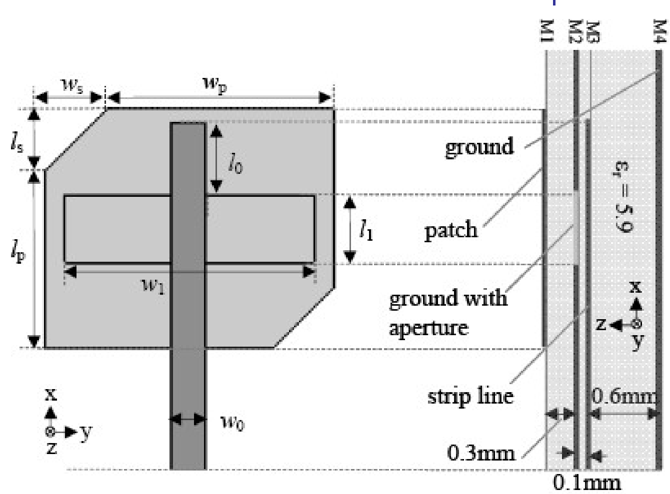

 80

Single CP Elements

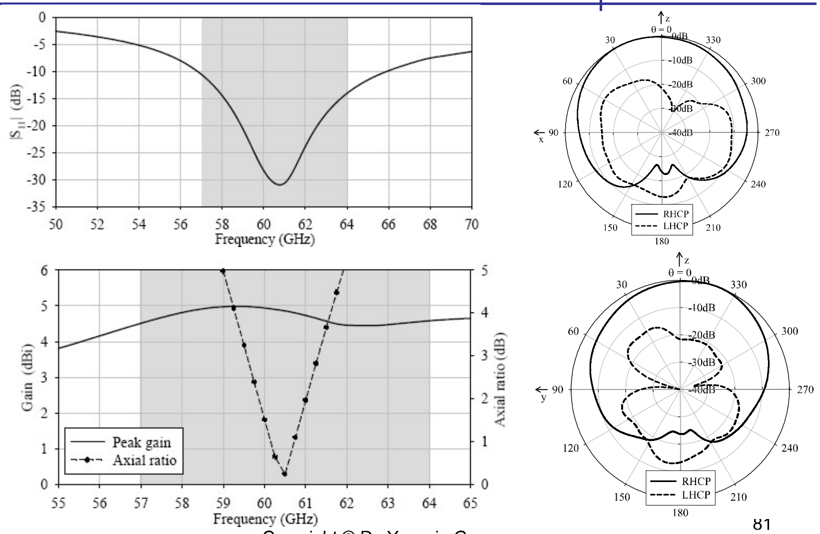

16-Element Array

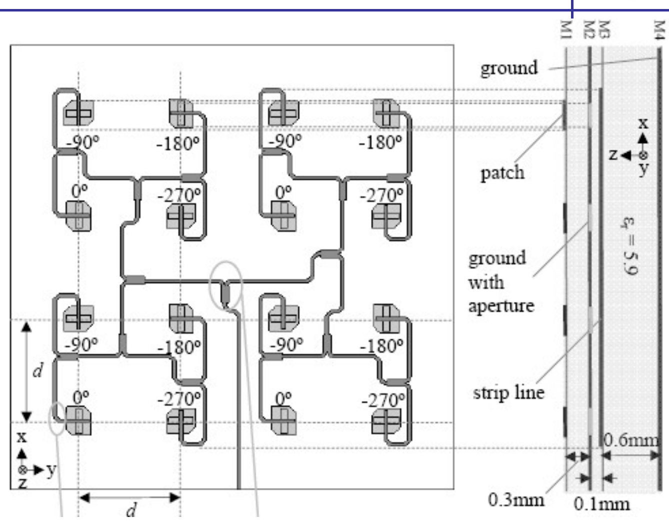

60-GHz CP Antenna Array

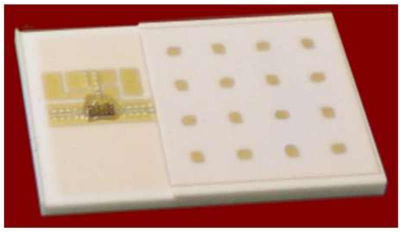

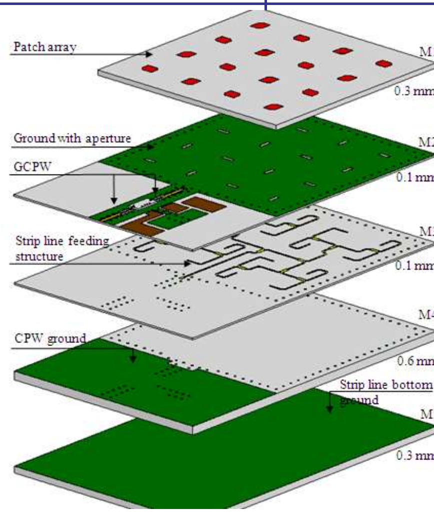

60-GHz CP Antenna Arrays

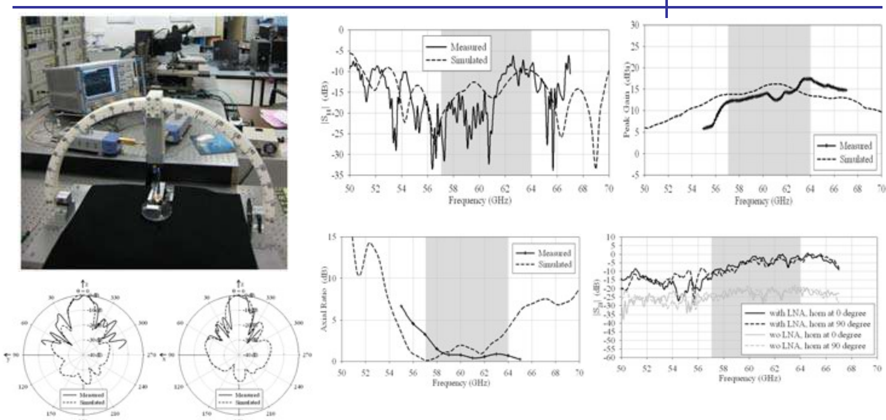

M. Sun, Y.Q. Zhang, **Y.X. Guo**, et al, Integration of Circular Polarized Array and LNA in LTCC as a 60-GHz Active Receiving Antenna, IEEE Trans Antennas and Propagation, vol. 59, no. 8, pp. 3083-3089, Aug 2011.

60-GHz SiP Radios

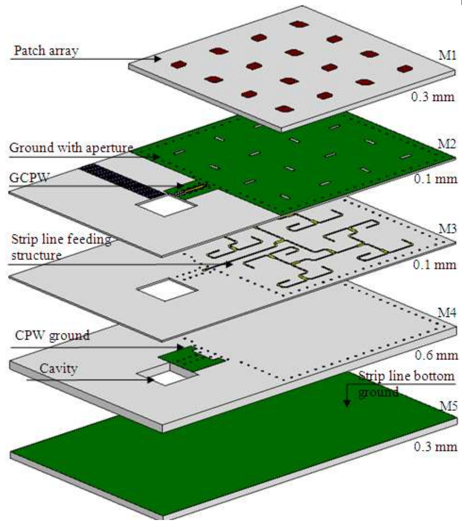

 85

60-GHz SiP and System Test

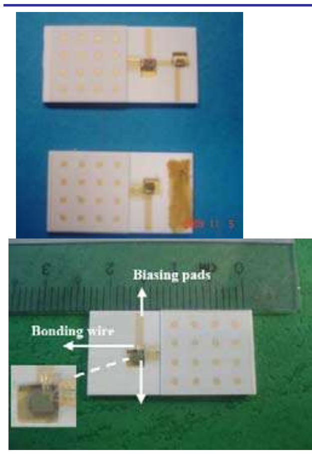

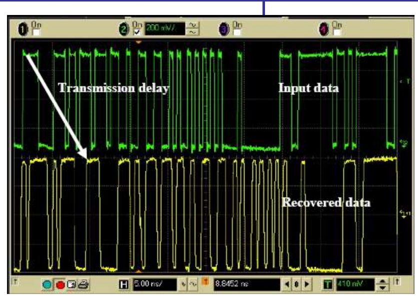

Transmitted and recovered data using the OOK modulator and 4x4 antenna array with a data rate of 2Gb/s

M.F. Karim, **Y.X. Guo**, et al., Integration of SiP Based 60GHz 4*4 Antenna Array with CMOS OOK Transmitter and LNA, IEEE Trans MTT, vol. 59, no.7, 2011, pp. 1869-1878.

 86

Single-Element Helical Antenna

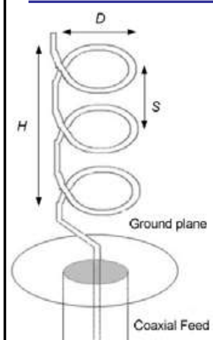

$$AR = \frac{|E_\theta|}{|E_\phi|} = \frac{2\lambda S}{(\pi D)^2}$$

$$\frac{2\lambda S}{(\pi D)^2} = \frac{2\lambda_g (3\times h4)}{(\pi\times 2\times r1)^2} \approx 0.695$$

$$AR = |\log_{10}^{0.695}| = 1.58\ dB$$

$$\frac{C}{\lambda} = \frac{2\times\pi\times r_1}{\lambda_g} \approx 0.915$$

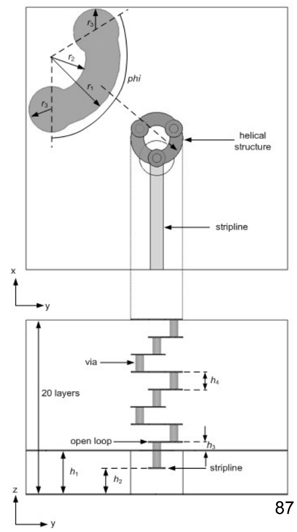

The proposed antenna element is composed of open loops at various layers connected by via holes to form an axial-mode helical structure to generate traveling wave radiation.

87

87

Single-Element Antenna

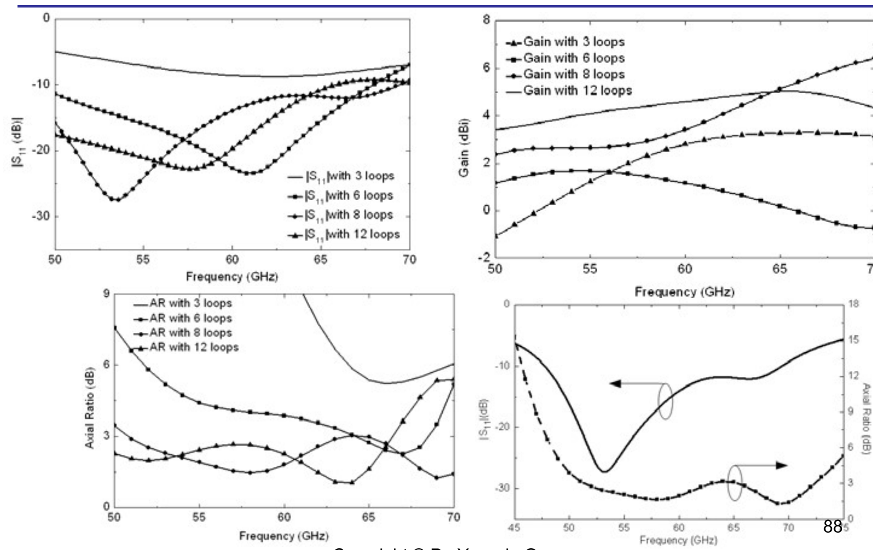

88

Slide 88

Tolerance Study

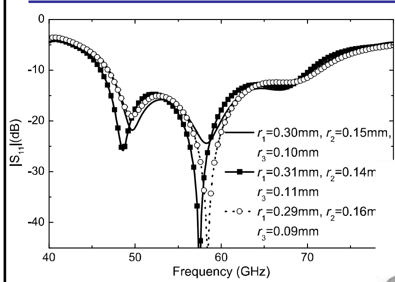

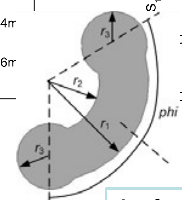

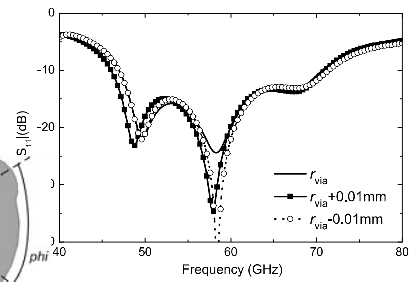

Shows the effect of the trace width variation. With a variation of ±0.01mm of r_1, r_2 and r_3, the antenna performance can be kept almost unchanged in the bandwidth.

As for the misalignment of via holes, catch pads have been used to enhance the electrical connection. With a change of ±0.01mm of radius of via holes, the antenna impedance bandwidth is also kept almost unchanged.

89

16-Element Antenna Array

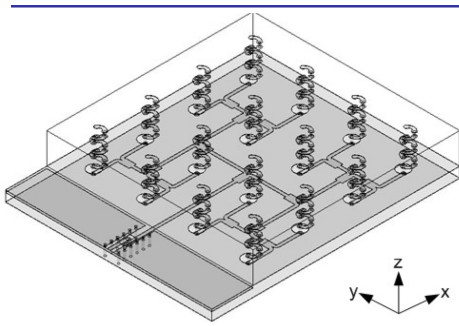

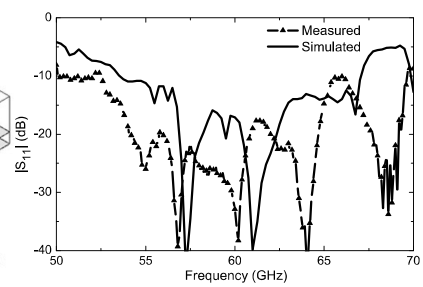

Composed of 16 antenna elements, T-junction feeding network and GCPW to stripline transition. Distance between neighboring elements is 2.5 mm and the size of this array is 12×10×2 mm^3.

Measured $|S_{11}|$ is less than -10 dB in the frequency range from 52.5 GHz to 65.5 GHz.

90

Slide 90

16-Element Antenna Array

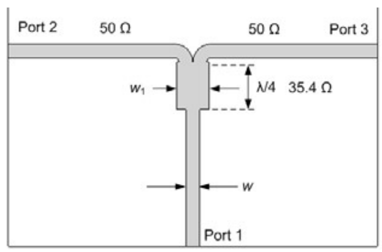

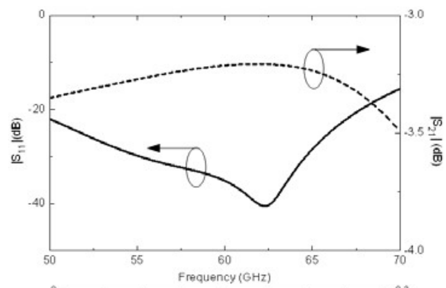

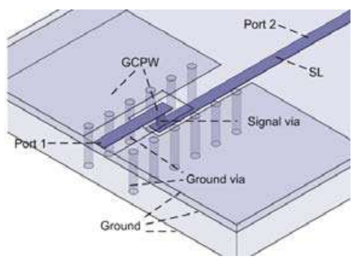

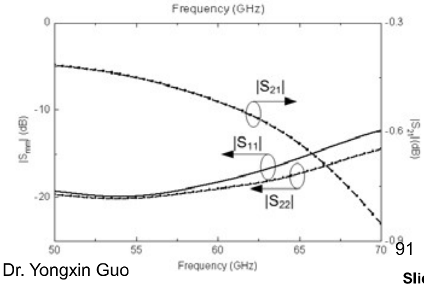

 91

Slide 91

16-Element Antenna

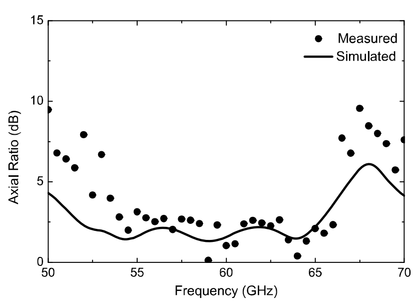

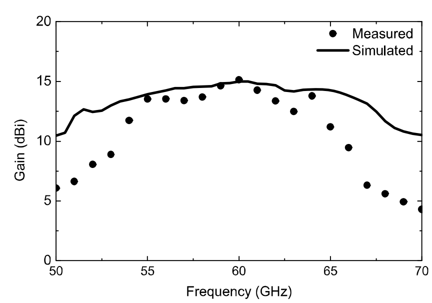

Measured AR is less than 3 dB in the frequency range from 54 GHz to 66 GHz.

C.R. Liu, Y.X. Guo, X.Y. Bao, S.Q. Xiao, 60-GHz LTCC Integrated Circularly Polarized Helical Antenna Array, IEEE Transactions on Antennas and Propagation, vol. 60, no.3, pp. 1329-1335, Mar 2012.

 92

Slide 92

16-Element Antenna

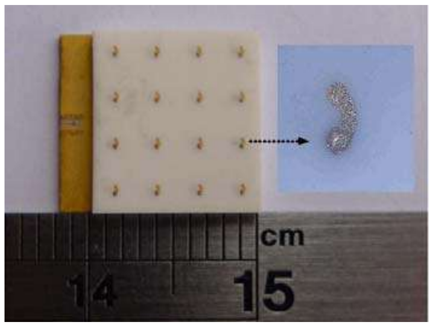

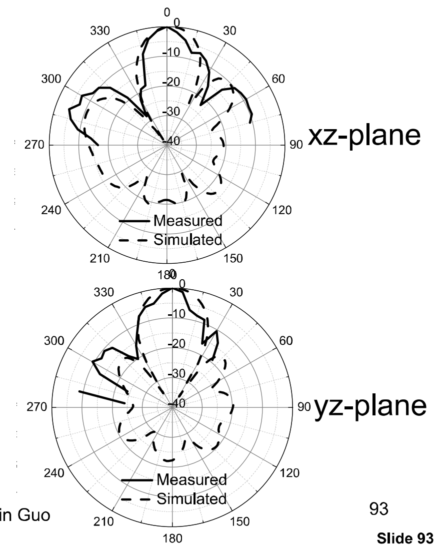

60-GHz Vertical Off-center Dipole Antenna

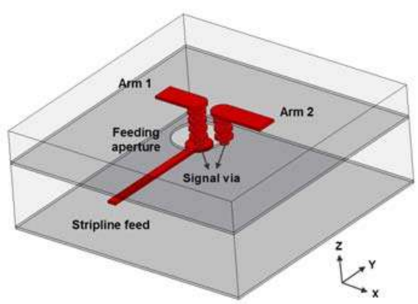

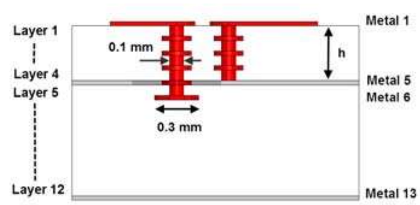

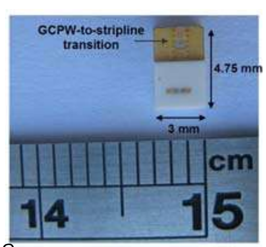

H. Chu, Y.X. Guo, Z.L. Wang, 60-GHz LTCC Wideband Vertical Off-Center Dipole Antenna and Arrays, IEEE Transactions on Antennas and Propagation, vol. 61, no.1, pp. 153-161, Jan 2013.

60-GHz Vertical Off-center Dipole Antenna

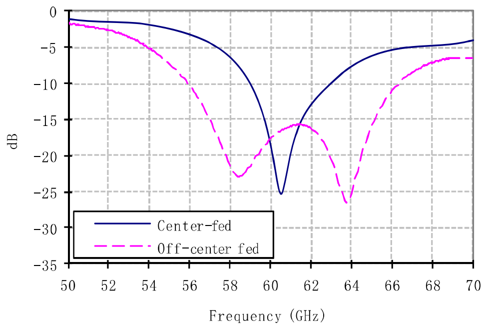

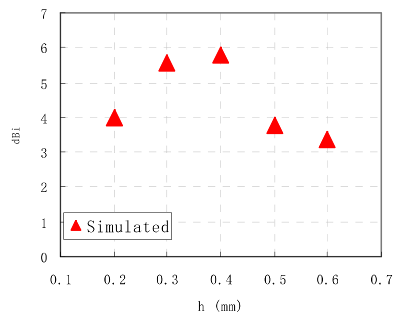

 95

60-GHz Vertical Off-center Dipole Antenna

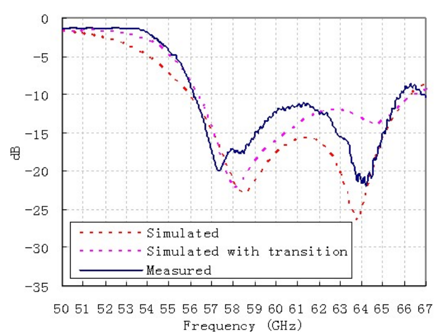

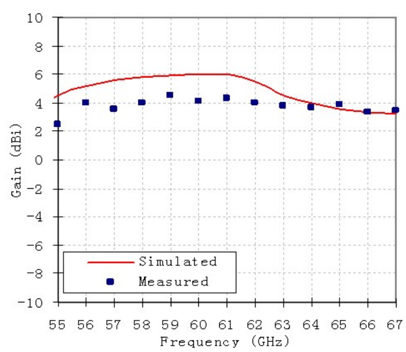

 96

60-GHz Vertical Off-center Dipole Antenna

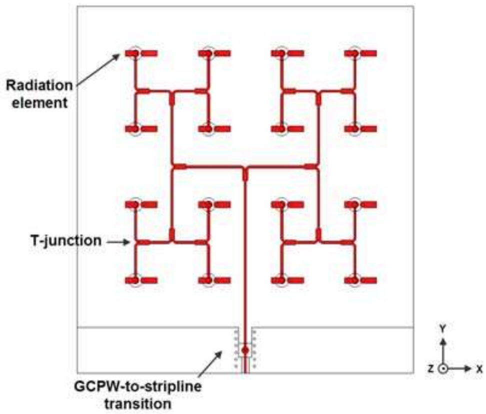

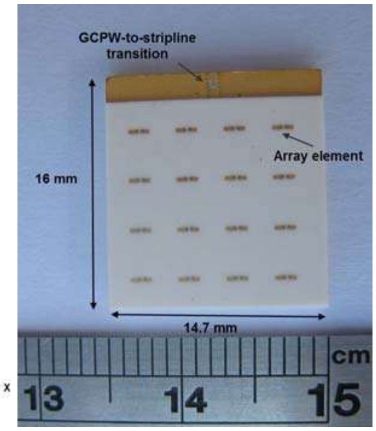

 97

60-GHz Vertical Off-center Dipole Antenna

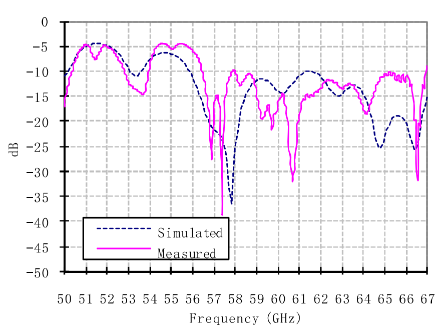

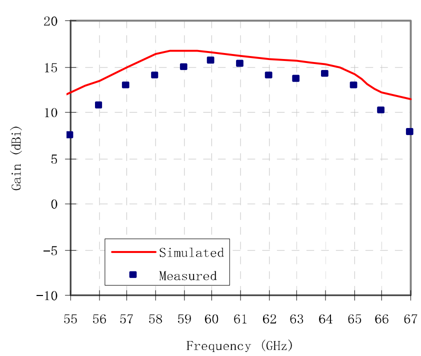

 98

60-GHz Vertical Off-center Dipole Antenna

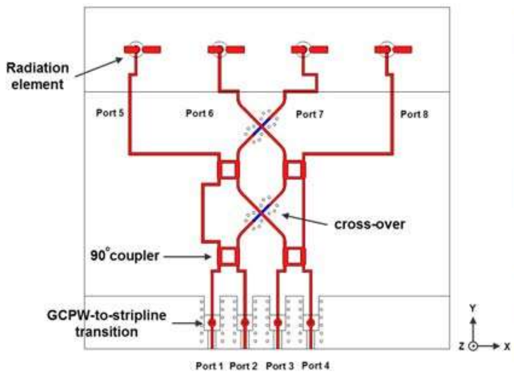

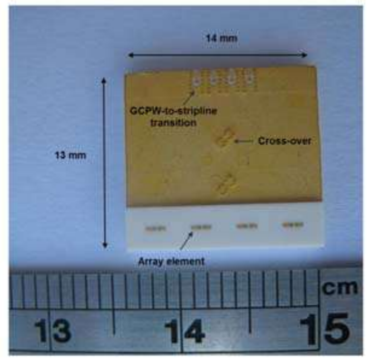

 99

60-GHz Vertical Off-center Dipole Antenna

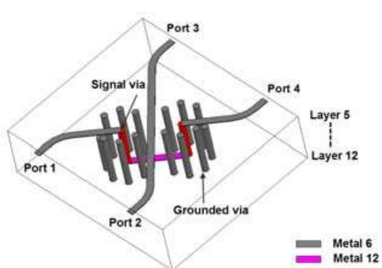

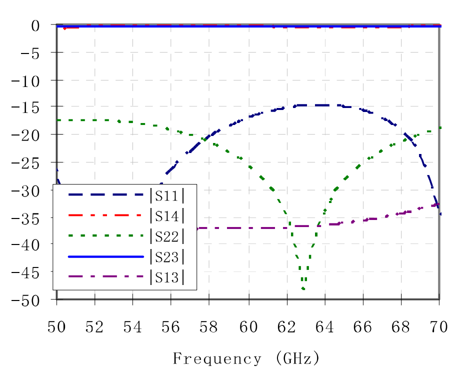

 100

60-GHz Vertical Off-center Dipole Antenna

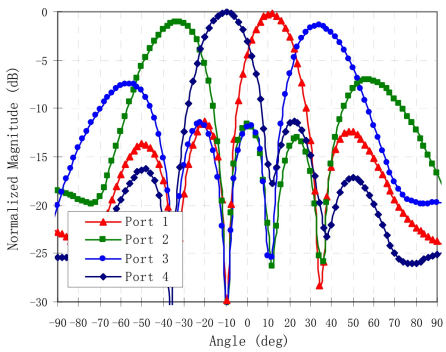

Simulated radiation pattern

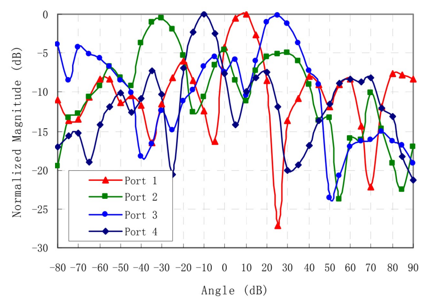

Measured radiation pattern

LTCC L-Probe Antenna

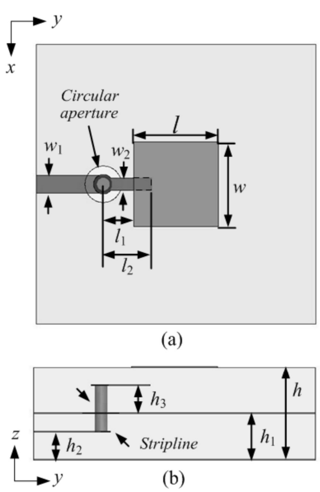

Para.	Dimensions (mm)	Para.	Dimensions (mm)
w	0.7	l	0.7
w_1	0.15	l_1	0.25
w_2	0.1	l_2	0.4
h	1	h_1	0.5
h_2	0.3	h_3	0.3

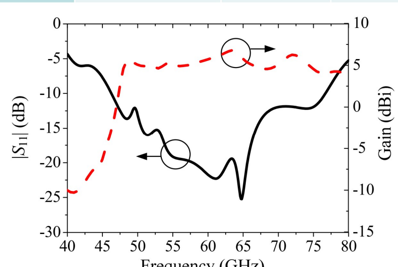

LTCC L-Probe Antenna with Soft-Surface

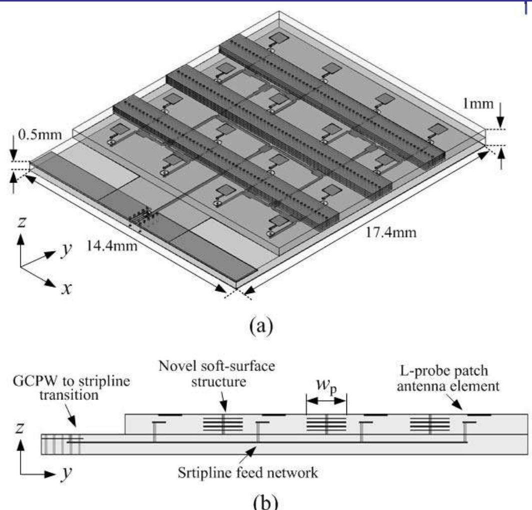

 103

Three LTCC L-Probe Antennas

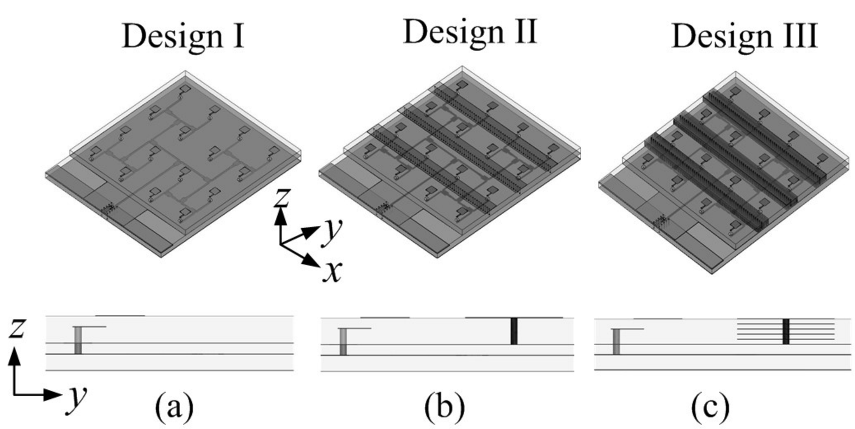

 104

Simulated Results for LTCC L-Probe Antennas

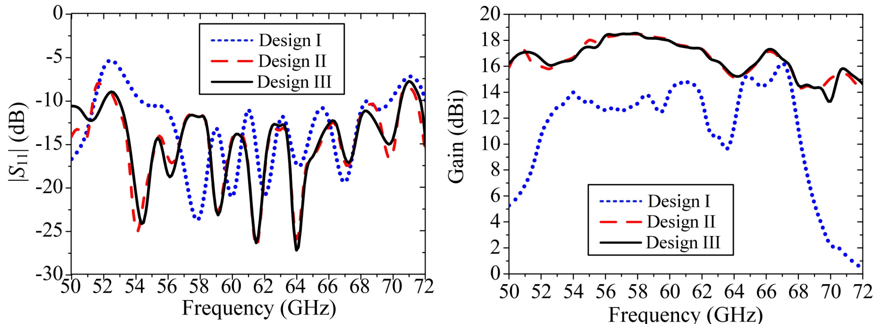

(a) (b)

LTCC L-Probe Antennas with 3 Different Soft-Surface

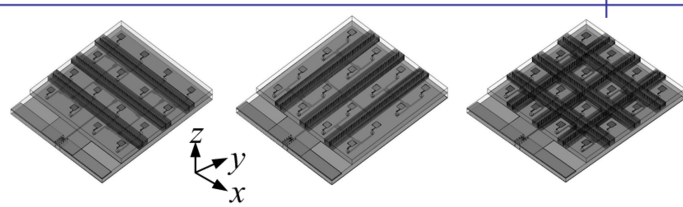

(a) (b) (c)

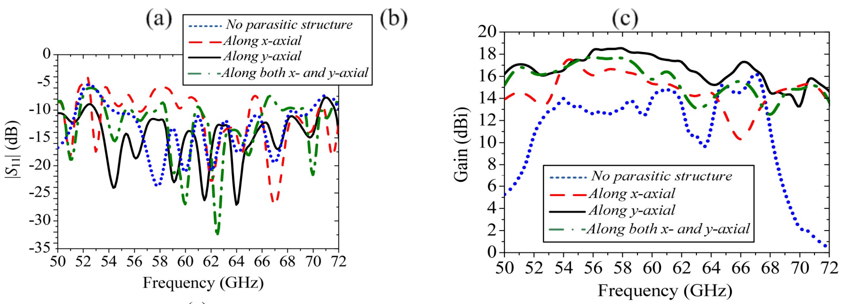

(a) (b)

LTCC L-Probe Antenna with Soft-Surface - Electrical Field Distributions

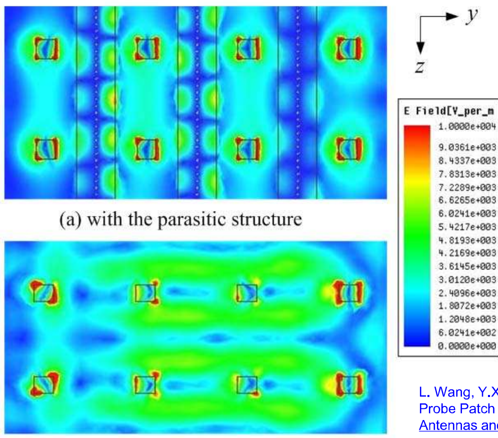

(a) with the parasitic structure

(b) without the parasitic structure

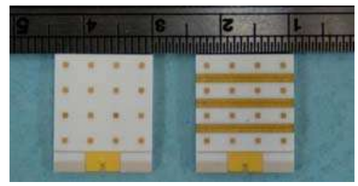

L. Wang, Y.X. Guo, W.X. Sheng, Wideband High-Gain 60-GHz LTCC L-Probe Patch Antenna Array with a Soft Surface, IEEE Transactions on Antennas and Propagation, vol. 61, no.4, pt1, pp. 1802-1809, Apr 2013.

60-Ghz Test Setup

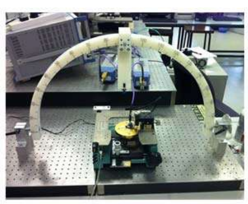

(a)

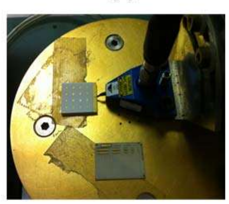

(b)

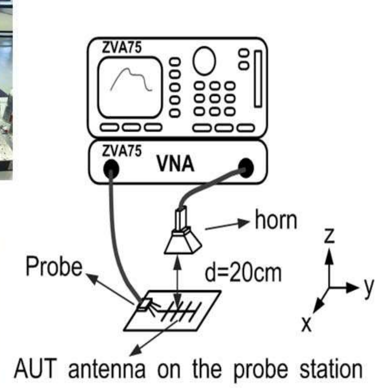

(c)

LTCC L-Probe Antennas with Soft-Surface - Simulated and Measured Results

Without Soft-Surface

With Soft-Surface

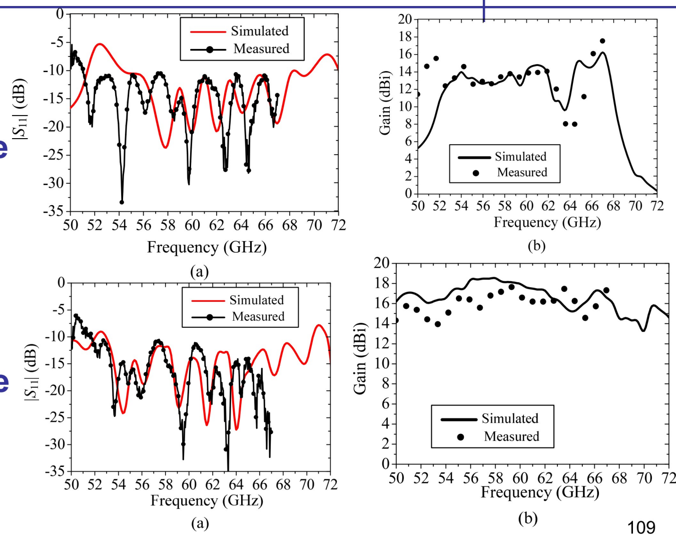

LTCC L-Probe Antenna with Soft-Surface - Comparison with Published Results

Type	Size & elements number	Impedance bandwidth	Gain
Grid array [20]	13.5×8×1.265 mm^3	14.8%	14.5 dBi
SIW fed Cavity array [20]	47×31×2 mm^3 8×8 elements	17.1%	22.1 dBi
Patch array with UC-EBG [21]	18.5×18.5 mm^2 4×4 elements	5.4%	18 dBi
Patch array with embedded-cavity [22]	18.6×18.6×0.6 mm^3 4×4 elements	5.8%	15.7 dBi
Patch array with open air cavities [26]	4×4 elements	14%	16.6 dBi
Our work	14.4×14.4×1 mm^3 4×4 elements	29%	17.5 dBi

LTCC L-Probe Antennas with Soft-Surface - Simulated and Measured Results

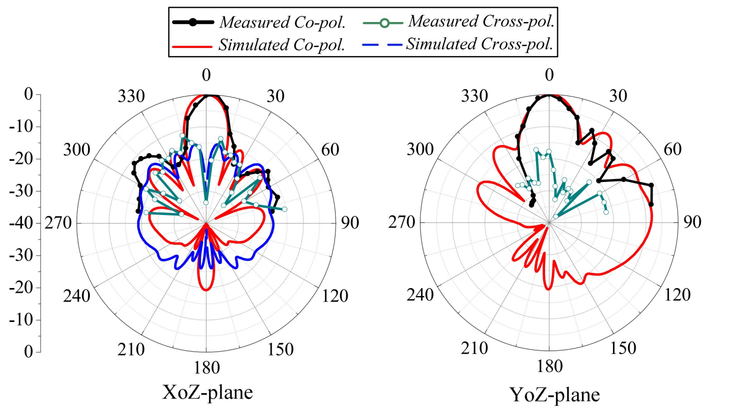

LTCC U-Slot Antenna

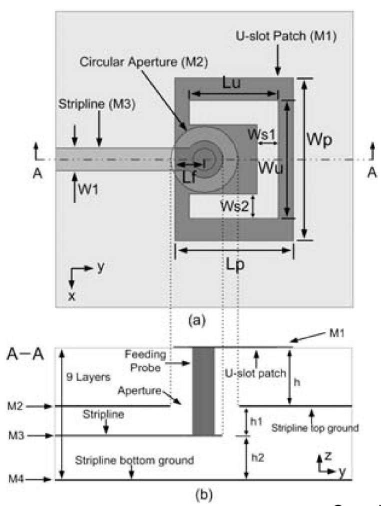

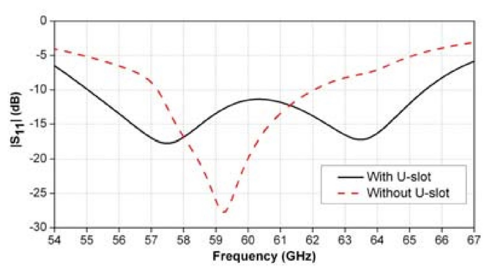

LTCC U-Slot Antenna Array

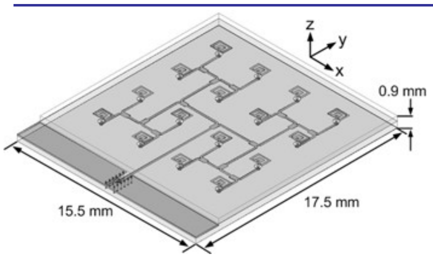

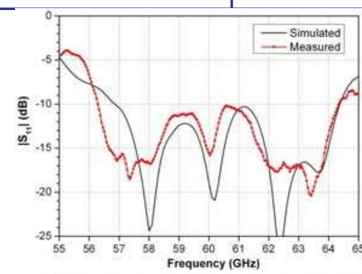

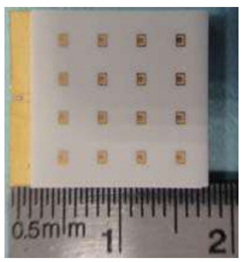

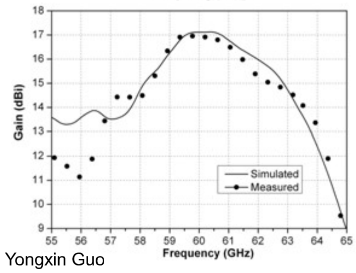

 113

LTCC U-Slot CP Antenna

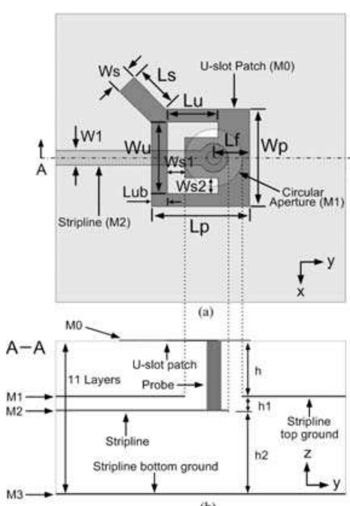

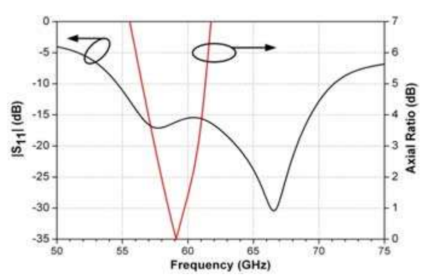

H.C. Sun, Y.X. Guo, Z.L. Wang, 60-GHz Circularly Polarized U-Slot Patch Antenna Array on LTCC, IEEE Transactions on Antennas and Propagation, vol. 61, no.1, pp. 430-435, Jan 2013.

 114

LTCC U-Slot CP Antenna Array

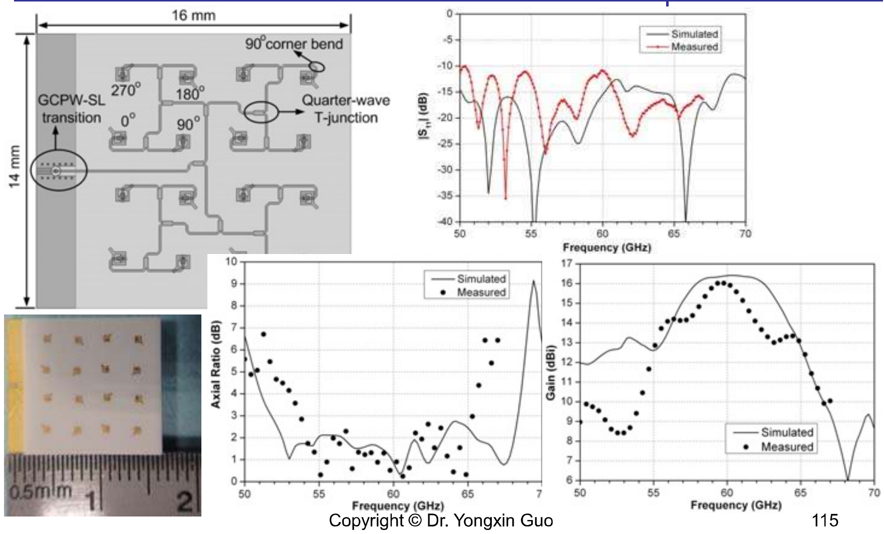

60-GHz Chip-Level Antennas

Typical CMOS Integrated Circuits

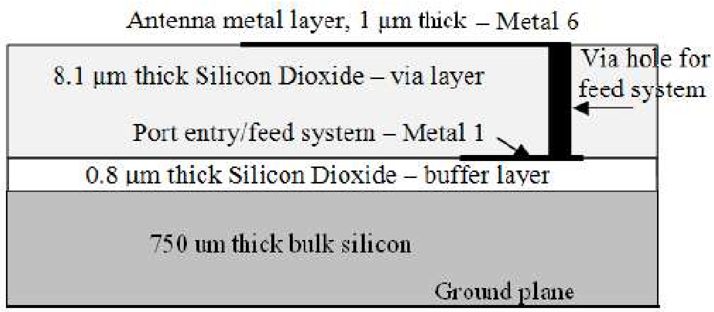

Illustration of IC modelling including silicon dioxide layer for a typical CMOS integrated circuit. Not to scale.

 117

State of Arts
- Inverted-F Antenna

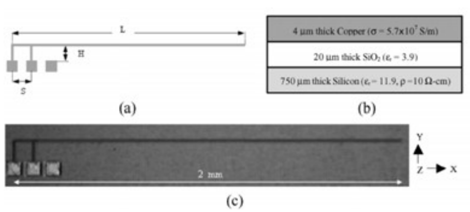

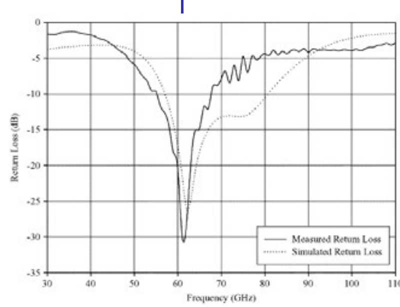

In the measurement, a gain of -19 dBi was obtained at 61 GHz for the inverted-F antenna; the simulated efficiency is 3.5%;

Y.P. Zhang, M. Sun, L.H. Guo, On-Chip Antennas for 60-GHz Radios in Silicon Technology, IEEE Trans on Electron DevicesJuly 2005, pp. 1664-1668.

 118

State of Arts
- Quasi-Yagi Antenna

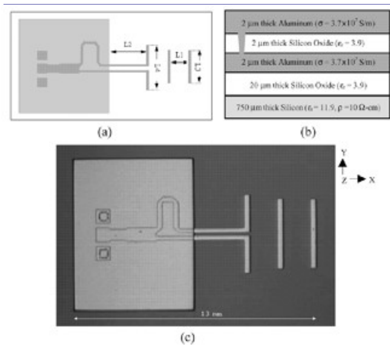

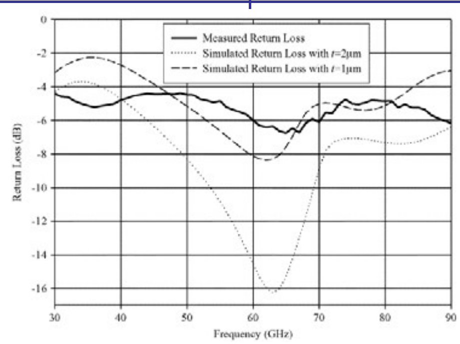

In the measurement, a gain of -12.5 dBi was obtained at 65 GHz for the quasi-Yagi antenna; the simulated efficiency is 5.6%;

Y.P. Zhang, M. Sun, L.H. Guo, On-Chip Antennas for 60-GHz Radios in Silicon Technology, IEEE Trans on Electron Devices, July 2005, pp. 1664-1668.

 119

State of Arts
- Using Standard CMOS Process

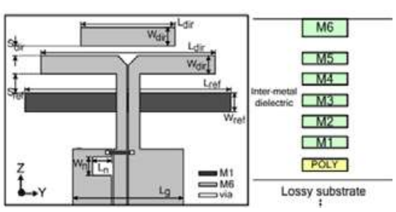

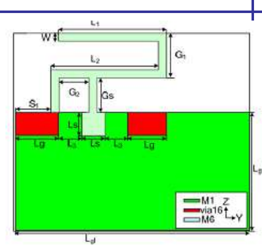

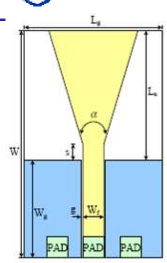

Type	Size (mm^2)	Simulated gain (dBi)	Measured gain (dBi)	BW	Efficiency
Yagi	1.1*0.95	-8	-10.6db	>10GHz	10%
Invert F	0.815*0.706	-13.82	-15.7db	>10GHz	10.2%
Monopole	1*0.81	-7.2	-9.4db	>10GHz	12%

Huey Ru-Chuang, et al, National Cheng Kung University, IEEE EDL, 06/2008

 120

60-GHz On-Chip Linearly Polarized Antennas

On-Chip Antennas using AMC

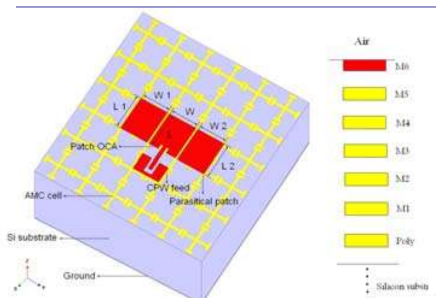

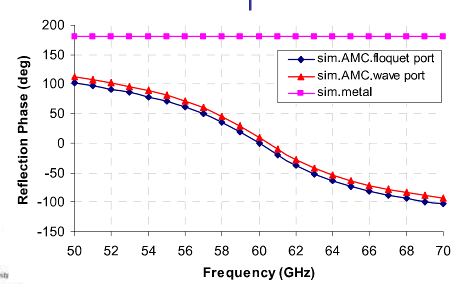

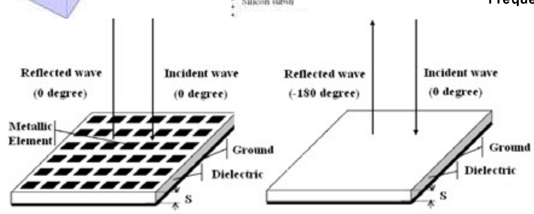

(a) (b)

On-Chip Antennas using AMC
- Current Distribution

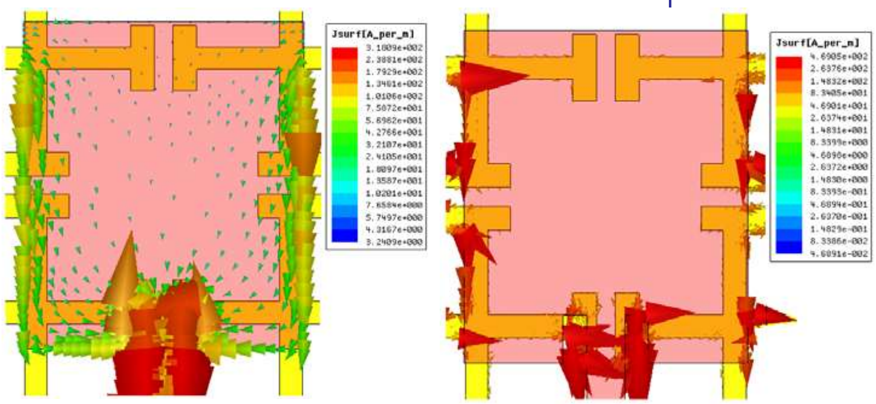

(a) Patch (b) AMC cells

 123

60-GHz Silicon On-Chip Antenna
- Measured and simulated |S11|

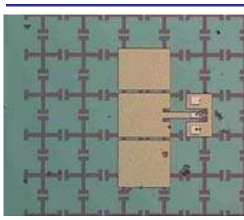

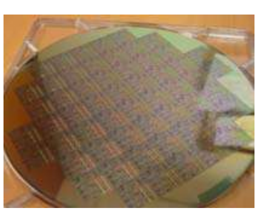

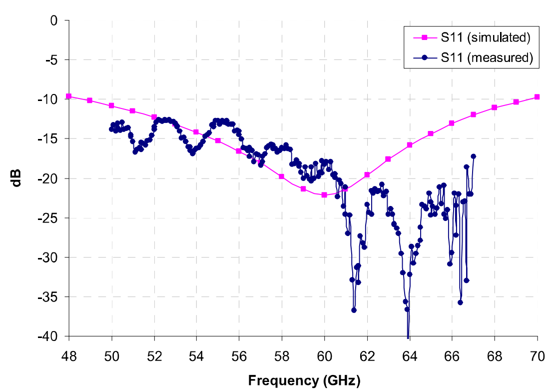

H. Chu, **Y.X. Guo**, X.Q. Shi, 60-GHz Broadband CMOS On-Chip Antenna with an Artificial Magnetic Conductor, IEEE Symposium on Radio Frequency Integration Technology 2009, Singapore, Dec 2009.

 124

60-GHz Silicon On-Chip Antenna
- Measured and simulated gain

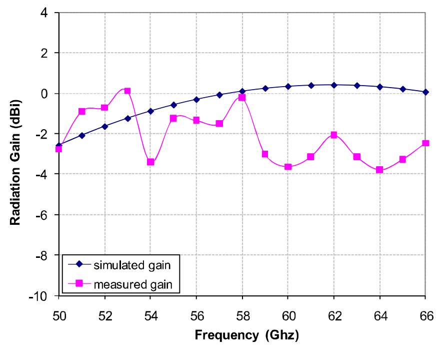

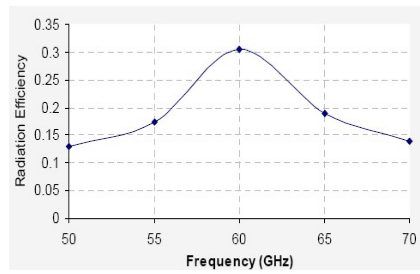

60-GHz Silicon On-Chip Antenna
- Radiation pattern at 60 GHz

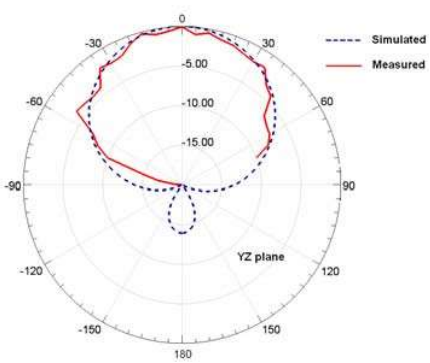

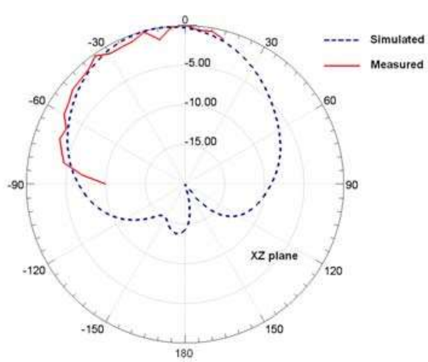

60-GHz On-Chip Circularly Polarized Antennas

 127

60-GHz On-Chip CP Antenna - AR and gain comparison

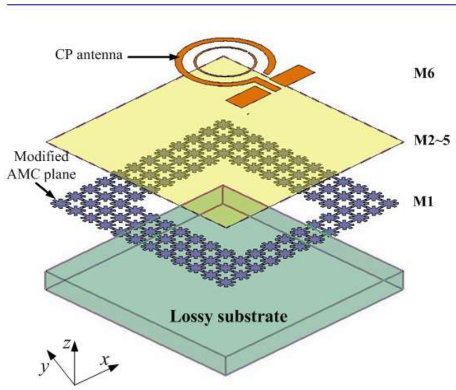

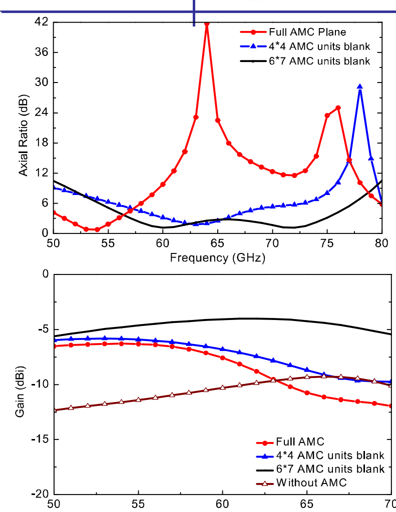

X.Y. Bao, Y.X. Guo, Y.Z. Xiong, 60-GHz AMC-Based Circularly Polarized On-Chip Antenna Using Standard 0.18-µm CMOS Technology, IEEE Transactions on Antennas and Propagation, vol. 60, no.5, pp. 2234-2241, May 2012.

 128

60GHz On-Chip CP Antenna without AMC - Single and double loops comparison

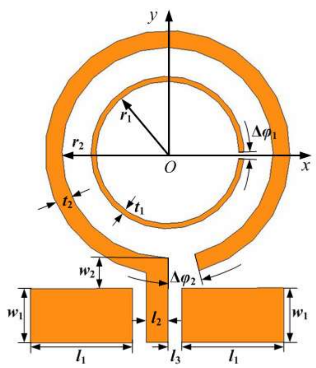

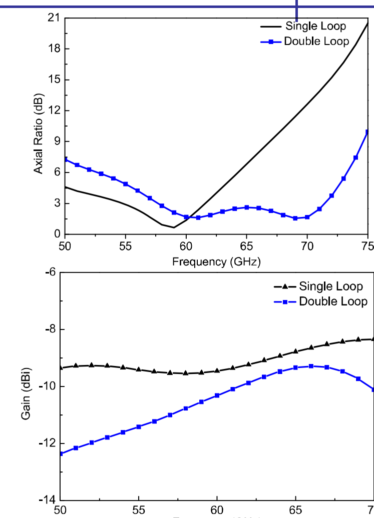

 129

60-GHz On-Chip CP Antenna - AMC parametric study

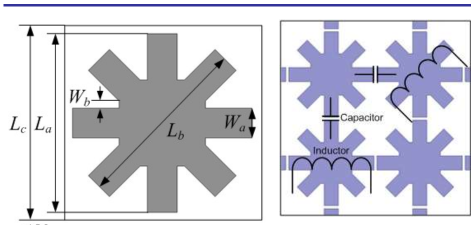

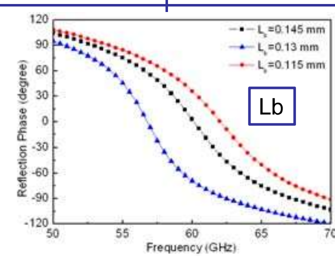

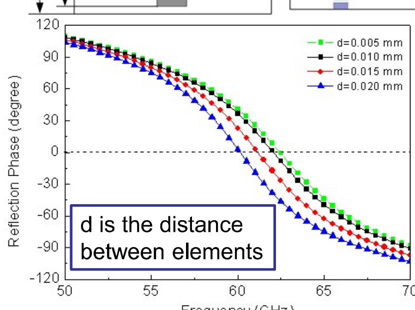

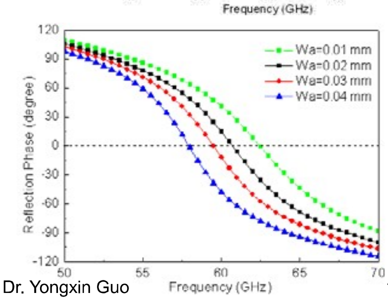

 130

60-GHz On-Chip CP Antenna - |S11|, AR and gain

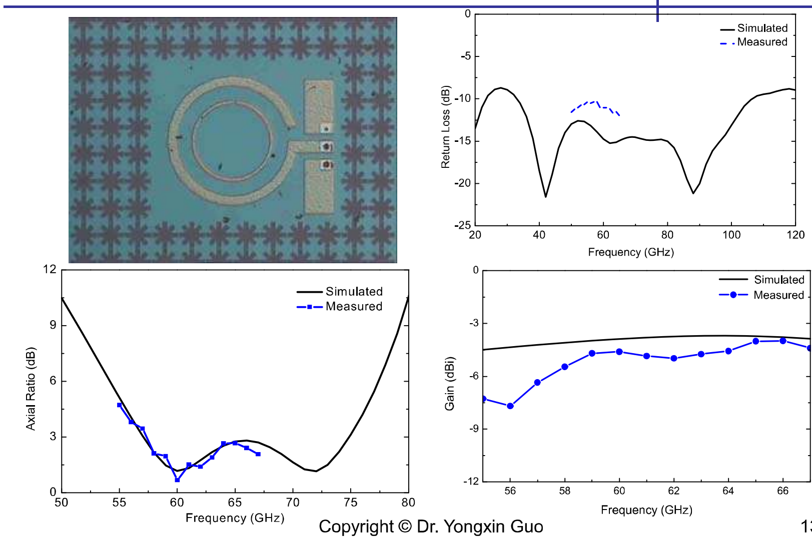

 131

60-GHz On-Chip CP Antennas - Gain and Radiation pattern

COMPARISON WITH PREVIOUSLY REPORTED 60GHZ CMOS ANTENNA

	Technology	Simulated Results in the Articles	Measured Power Gain	Polarization
Qusi-Yagi[3]	Post-back-end-of-line	NA	-12.5 dBi@65 GHz	Linearly Polarized
Invert-F[3]	Post-back-end-of-line	NA	-19 dBi@61 GHz	Linearly Polarized
Monopole[4]	0.18-um CMOS	-7.2 dBi	-9.4 dBi	Linearly Polarized
Yagi [5]	0.18-um CMOS	-8 dBi	-10.6 dBi	Linearly Polarized
Meander-line-Invert–F [6]	0.18-um CMOS	-13.82 dBi	-15.7 dBi	Linearly Polarized
Our work	0.18-um CMOS	-3.7 dBi	-4.4 dBi@65Ghz	Circularly Polarized

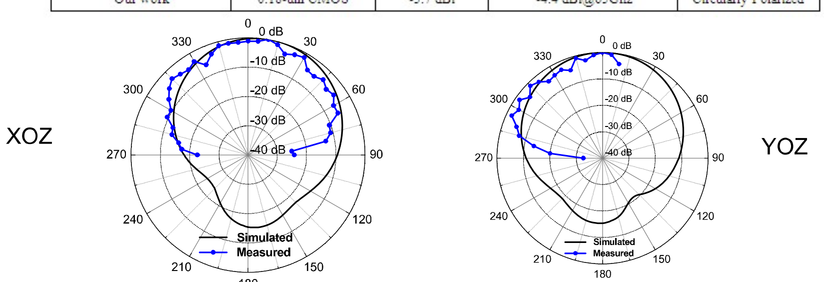

 132

60-GHz Indoor Communications - Link Budget Analysis

The transmission distance and the overall Tx and Rx antenna gain for a QPSK communication link with a data rate of 2 Gbps:

$$G_T + G_R = 2 + C/N + 20\log d$$

- G_T and G_R are the Tx and Rx antenna gain;
- The carrier-to-noise ratio C/N required for QPSK modulation is 10.7 dB.
- d is the distance between Tx and Rx in meter.

Findings:

(1) Overall Tx and Rx gain ($G_T + G_R$) of 12.7 dB can deliver 1-meter distance.

(2) If the distance is 10 meter (indoor communications), the required overall Tx and Rx gain ($G_T + G_R$) is of 32.7 dBi.

(3) It is not very difficult to have antenna gain of 15 dBi for a Tx antenna array.

(4) For our on-chip antenna case, if the Tx/Rx antenna gain are 15 dBi and -4.4 dBi, respectively, then the achieved distance for the QPSK is

$$d = 10^{(G_T + G_R - 2 - C/N)/20} = 0.785 \text{ meter}$$

 133

Innovative CMOS process: Wafer Transfer Technology

Wafer Transfer Technology (WTT): The microwave device pattern was first fabricated on the Si substrate using the microelectronic technology, and then the pattern was transferred to the low-loss microwave substrate.

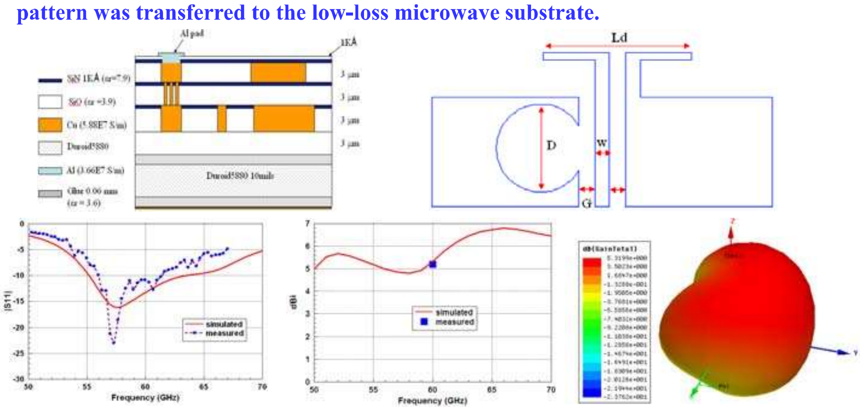

Y.X. Guo, J.P. Wang, B. Luo, E.B. Liao, Development of A 60 GHz Band Pass Filter and A Dipole Antenna using Wafer Transfer Technology, IEEE Electron Device Letters, vol. 30, no.7, pp. 784-786, July 2009. 134

Micromachined Sub-THz On-Chip Antennas

135-GHz On-Chip Antenna - Monopole

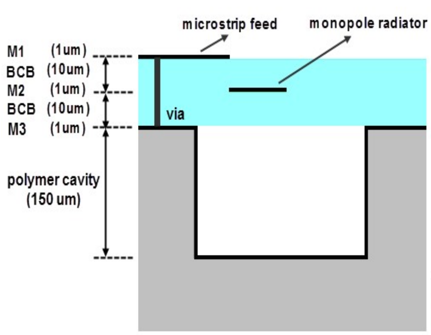

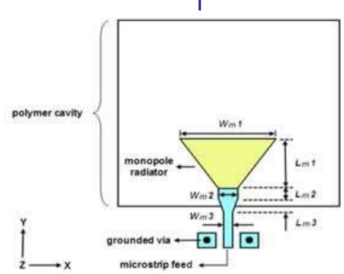

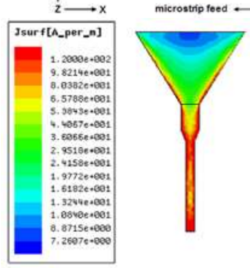

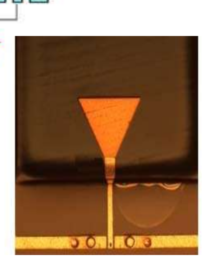

H Chu , Y.X. Guo, et al, 135-GHz Micromachined On-chip Antenna and Antenna Array, IEEE Transactions on Antennas and Propagation, vol. 60, no. 10, pp. 4582-4588, Oct 2012.

135-GHz On-Chip Antenna - Fabrication process

3 main steps:
1) cavity fabrication,
2) polymer cavity filling
3) pattern formation through back-end-of-line (BEOL) process; 2 redistribution layers (RDLs) are required.

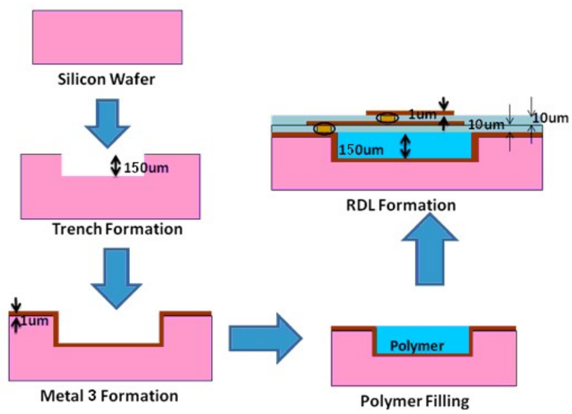

135-GHz On-Chip monopole antenna - |S11|, gain and radiation pattern

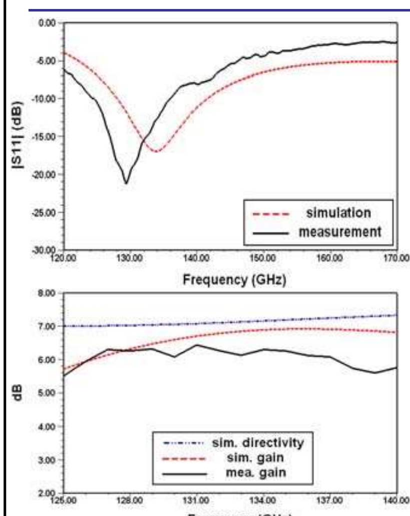

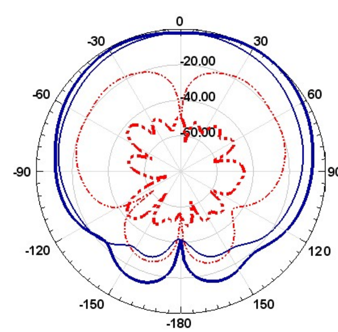

135-GHz On-Chip Antenna - 2*1 patch array

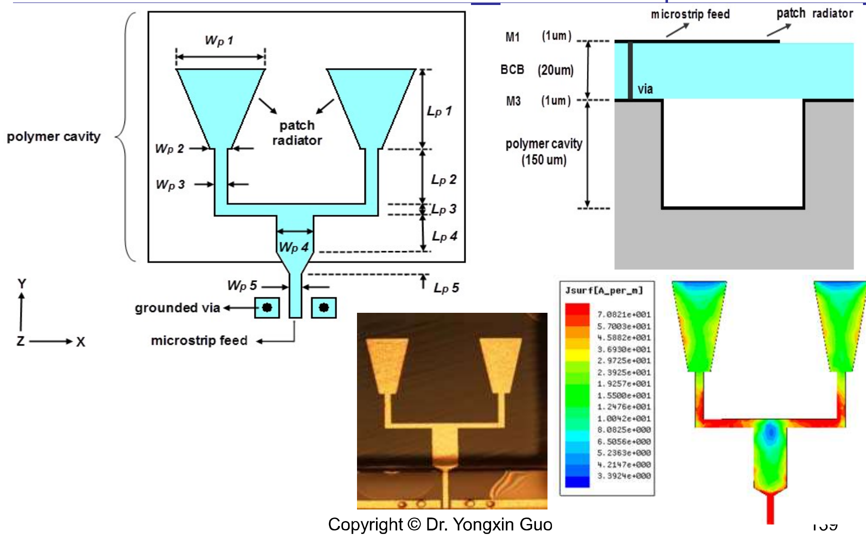

135-GHz On-Chip Patch Antenna - 2*1 patch array

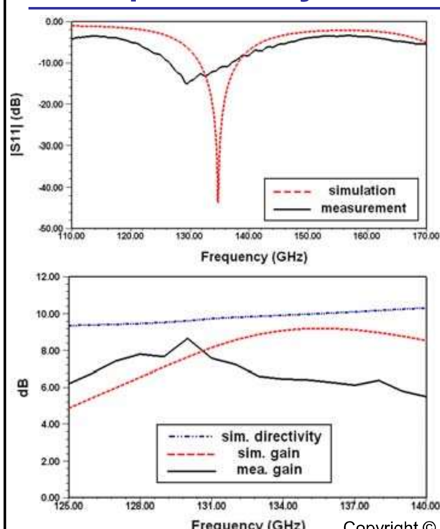

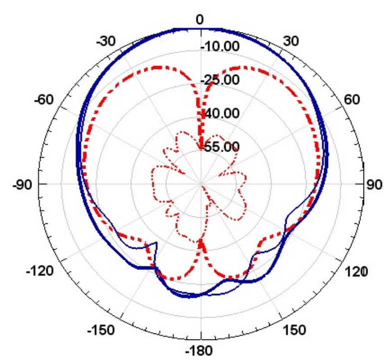

140

MMIC Modelling and Design

1. **Small Signal and large signal modeling**
2. **High-power Ku-/Ka-band Power amplifier on GaAs/GaN**
3. **60/94 GHz power amplifier/LNA**

- Z. Zhong, Y.X. Guo, M.S. Leong, A Consistent Charge Model of GaAs MESFETs for Ku-band Power Amplifiers, IEEE Transactions on Microwave Theory and Technique, vol. 59, no. 9, pp. 2246-2253, Sept 2011.
- Y.S. Long, Y.X. Guo, Z. Zhong, A 3-D Table-Based Method for Non-Quasi-Static Microwave FET Devices Modeling , IEEE Transactions on Microwave Theory and Techniques, vol. 60, no. 10, pp. 3088-3095, Oct 2012.
- X.J. Bi, Y.X. Guo, et al, "A 60 GHz 1 V-Supply Band-tunable Power Amplifier in 65 nm CMOS", IEEE TRANSACTIONS ON CIRCUITS AND SYSTEMS II-EXPRESS BRIEFS,Volume: 58, Issue: 11,Pages: 719-723 NOV 2011.
- X.J. Bi, Y.X. Guo, Y.Z. Xiong, M.A. Arasu, M. Je, "A 19.2 mW, >45 dB gain and high-selectivity 94 GHz LNA in 0.13 um SiGe BiCMOS," IEEE Wireless and Components Letters, vol. 23, no.5, pp. 261-263, May 2013
- X.J. Bi, Y.X. Guo, M. Je, Analysis and Design of Gain Enhanced Cascode Stage Utilizing a New Passive Compensation Network, IEEE Transactions on Microwave Theory and Techniques, vol. 61, no. 8, pp. 2892-2990, Aug 2013.
- K. Kang, F. Lin, D. Pham, J. Brinkhoff, C.H. Heng, Y.X. Guo, X.J. Yuan, A 42-mW 60-GHz OOK Receiver with an On-chip Antenna in 90nm CMOS, IEEE Journal of Solid-State Circuits (JSSC), Vol. 45, No. 9, pp. 1720-1731, Sept 2010.
- L. Wang, Y.X. Guo, Y. Lian, C.H. Heng, 3~5GHz 4-Channel UWB Beamforming Transmitter with 1° Phase Resolution through Calibrated Vernier Delay Line in 0.13μm CMOS, IEEE International Solid-State Circuits Conference 2012 (ISSCC2012), USA.

 141

0.18 um GaAs MESFETs Process Device Modelling

 142

0.18 um GaAs MESFETs Wafer Device Small-signal Modelling

8*150 um GaAs MESFET wafer device
V_{gs} = -0.3V, V_{ds} = 7V, 1 – 40GHz

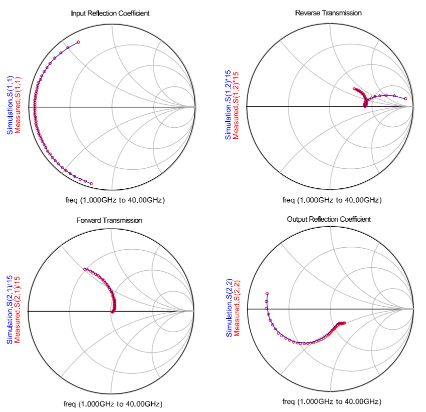

16*150 um GaAs MESFET wafer device
V_{gs} = -0.3V, V_{ds} = 7V, 1 – 40GHz

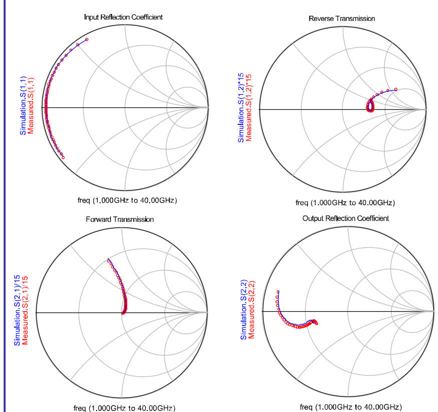

0.18 um GaAs MESFETs Wafer Device Large-signal Modelling

6×125 um GaAs MESFET wafer device
V_{gs} = -3.1 – 0.5V, V_{ds} = 0 – 10V

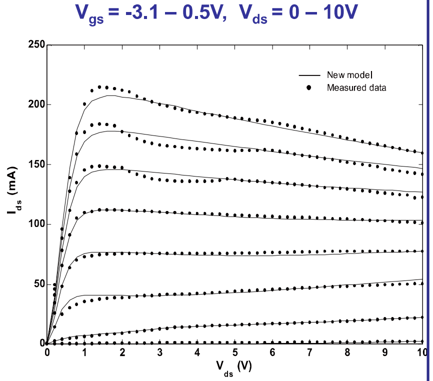

16×125 um GaAs MESFET wafer device
V_{gs} = -3.1 – 0.5V, V_{ds} = 0 – 10V

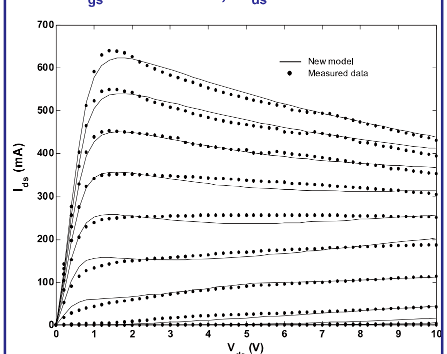

Z. Zhong, **Y.X. Guo**, M.S. Leong, A Consistent Charge Model of GaAs MESFETs for Ku-band Power Amplifiers, IEEE Transactions on Microwave Theory and Technique, vol. 59, no. 9, pp. 2246-2253, Sept 2011.

ADS Design Kit for 0.18 um GaAs MESFETs Wafer Device

- First open "Advanced Design System", choose "DesignKit" → "Intall design kits",

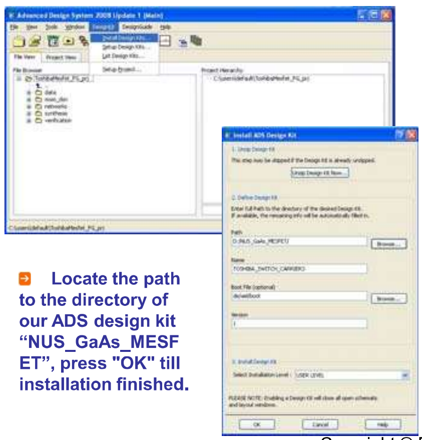

- Locate the path to the directory of our ADS design kit "NUS_GaAs_MESFET", press "OK" till installation finished.

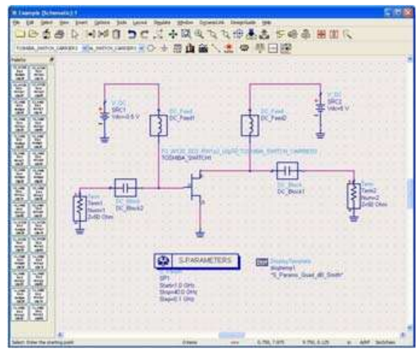

- All the GaAs MESFETs can be found as available design components in palette area of ADS.

 145

Load-Pull Measurement Setup

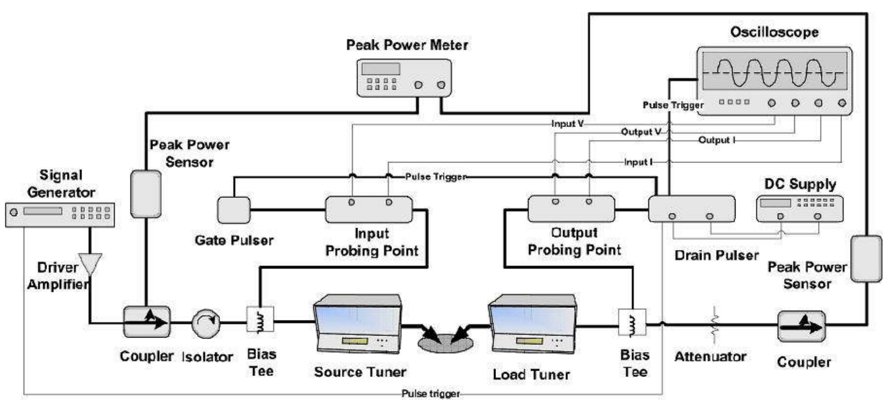

 146

Load-Pull Measurement Setup

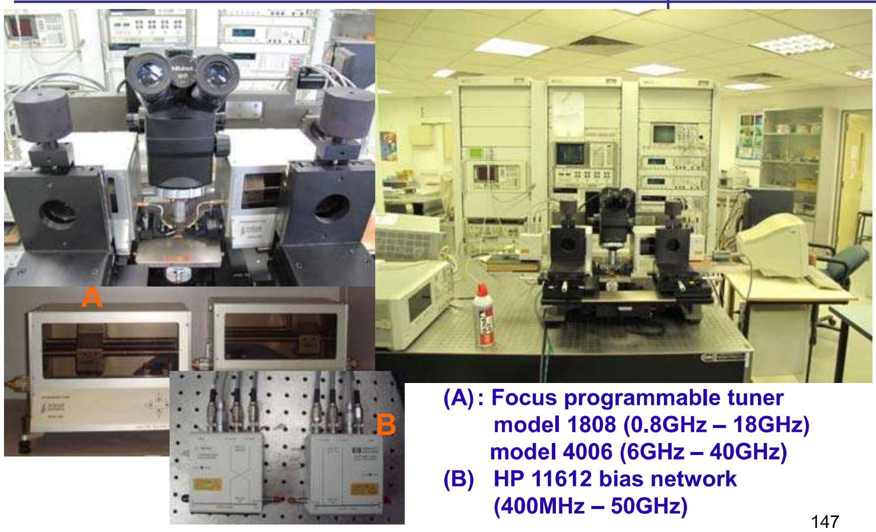

(A) : Focus programmable tuner
model 1808 (0.8GHz – 18GHz)
model 4006 (6GHz – 40GHz)
(B) HP 11612 bias network
(400MHz – 50GHz)

147

Load-Pull Measurement Verification (1)

8x100um 33GHz V_{gs}=-0.6V, V_{ds}=5.0V

	Source Impedance	Load Impedance	Gain
Measurement	9.07 – j*1.80 Ohm	12.223 + j*13.22	6.37
ADS Simulation	9 - j*1.8 Ohm	12.247 + j*12.06	6.45

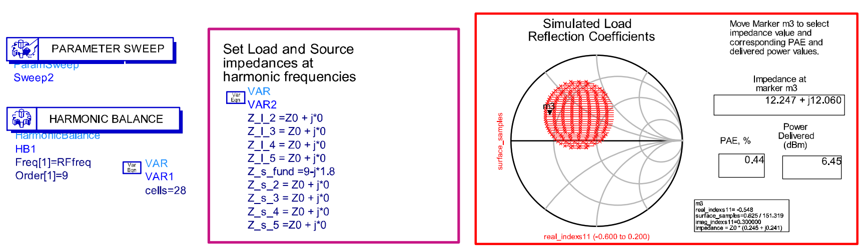

148

Load-Pull Measurement Verification (2)

8x75um 33GHz V_{gs}=-0.6V, V_{ds}=5.0V

	Source Impedance	Load Impedance	Gain
Measurement	9.07 – j*1.80 Ohm	13.3745+j*22.9913	7.45
ADS Simulation	9 - j*1.8 Ohm	12.418 + j*23.750	7.50

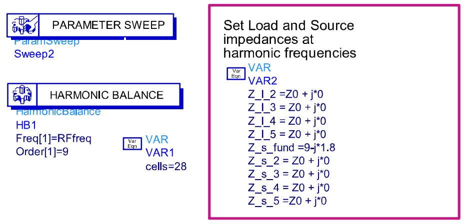

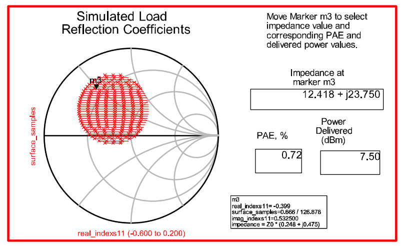

 149

11.5 – 15.0 GHz GaAs MESFET MMIC Power Amplifier

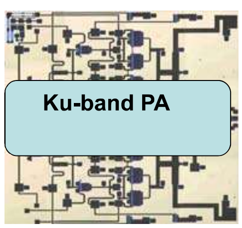

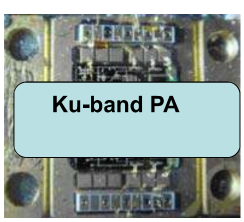

ELECTRICAL SPECIFICATION REV.YEAR 2007

No.	Item	Symbol	Unit	Value min.	Value typ.	Value max.	
1-1	Frequency	---	MHz	11,500	---	15,000	
2-1	P1dB (over Frequency)	P1dB	dBm	35	36	---	at the 1dB compression gain Tambient = +25 degC
3-1	P_{out} Flatness	---	dB_{p-p}	---	±1	---	P1dB Tambient = +25 degC
4-1	Small signal gain	Gss	dB	24.8	25	26.3	Pout = + 20.0 dBm Tambient = +25 degC
5-1	P_{out} Variation over V_{DD}	---	dB/V	---	---	0.3	P_{in} = + 8.0 dBm Tambient = +25 degC
6-1	Input Return Loss	S11	dB	12	---	---	
7-1	Output Return Loss	S22	dB	6	---	---	
8-1	Die's SIZE	SQUER	MM^2			5X5	
9-1	2^{nd} & 3^{rd} Harmonics	---	dBc	---	---	-20	
10-1	Undamaged Output Load VSWR	---	---	---	---	2.0 : 1	
11-1	K-factor upto 40GHz	K	---	1	---	---	Frequency Range : upto 40GHz
12-1	DC Drain Current (Peak)	I_{DD}	mA	---	4,200	4,800	
13-1	IC Process						
14-1	DC Gate Current	I_{GG}	mA	---	---	40	

 150

11.5 – 15.0 GHz Power Amplifier Measured Data

Biasing Condition
V_{gs} = -0.3V, V_{ds} = 6V

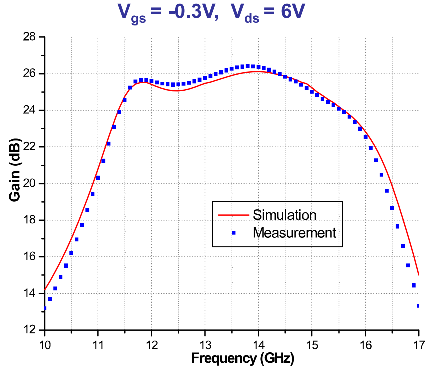

P_{in}-P_{out} @ 13 GHz

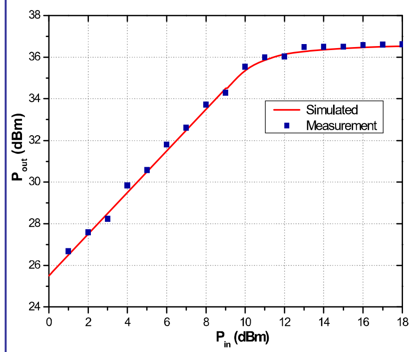

Z. Zhong, **Y.X. Guo**, M.S. Leong, A Consistent Charge Model of GaAs MESFETs for Ku-band Power Amplifiers, IEEE Transactions on Microwave Theory and Technique, vol. 59, no. 9, pp. 2246-2253, Sept 2011.

60 GHz Power Amplifier Measured Data

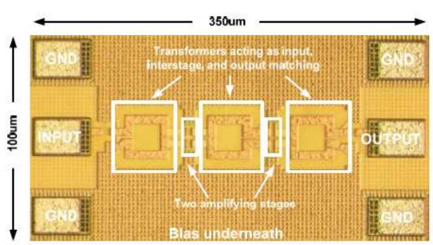

This work received the "Best Student Paper Award" in International Conference on Microwave and Millimeter-Wave Technology 2010 (ICMMT2010) at Chengdu, China, May 8-11, 2010.

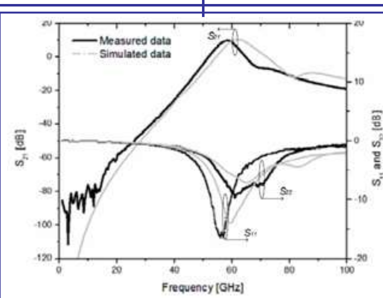

Peak gain Freq.	**58.5 GHz**
Peak gain:	**10.1 dB**
DC power:	**52 mW**
OP1dB:	**5.1 dBm**
P_{sat}	**8.5 dBm**
Peak PAE:	**7.7%**
Stages:	**2**
V_{DD}:	**1 V**
Technology:	**90 nm CMOS**

60 GHz Band-Tunable Power Amplifier Measured data

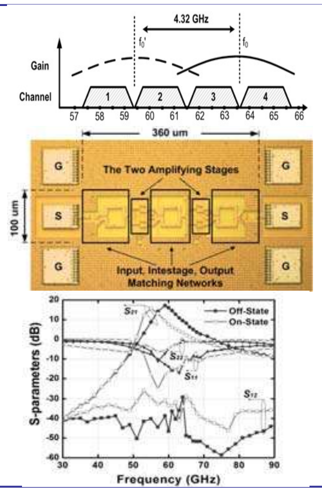

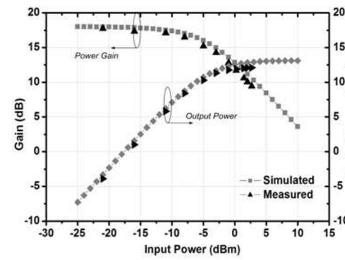

Peak gain Freq.	**59 GHz**
Peak gain:	**17.1 dB**
DC power:	**63 mW**
P_{sat}	**12.3 dBm**
Peak PAE:	**20.4%**
Stages:	**2**
V_{DD}:	**1 V**
Technology:	**65 nm CMOS**

X.J. Bi, **Y.X. Guo**, et al, "A 60 GHz 1 V-Supply Band-tunable Power Amplifier in 65 nm CMOS", IEEE TRANSACTIONS ON CIRCUITS AND SYSTEMS II-EXPRESS BRIEFS, Volume: 58, Issue: 11,Pages: 719-723 NOV 2011.

 153

94-GHz Low Noise Amplifier Measured data

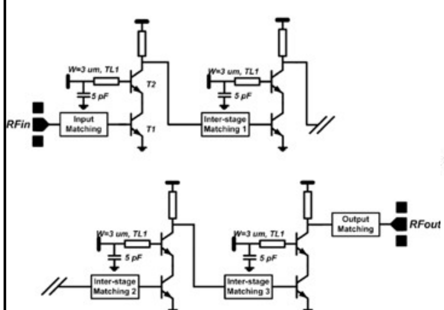

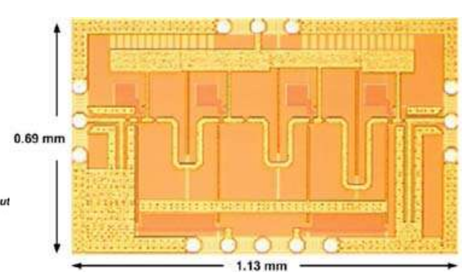

X.J. Bi, **Y.X. Guo**, Y.Z. Xiong, M.A. Arasu, M. Je, "A 19.2 mW, >45 dB gain and high-selectivity 94 GHz LNA in 0.13 um SiGe BiCMOS," IEEE Wireless and Components Letters, vol. 23, no.5, pp. 261-263, May 2013

 154

94-GHz Low Noise Amplifier Measured data

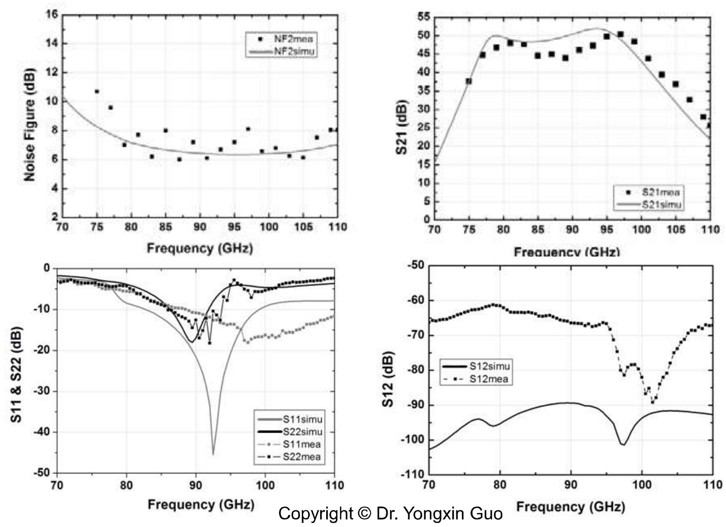

 155

New passive devices: Ka-Band SIW BPF (PCB); X-Band Balun BPF (PCB); 60-GHz LTCC BPF (LTCC); 40/50-GHz LTCC diplexer (LTCC); Use of Space Mapping to optimize two SIW BPFs (PCB); Ka-Band Triplexer (LTCC)

- J.P. Wang, Y.X. Guo, B.Z. Wang, L.C. Ong, High-selectivity dual-band stepped-impedance bandpass filter, Electronics Letters, vol.42, no.9, April 2006, pp. 538-539.
- J.P. Wang, J. Ni, Y.X. Guo, D.G. Fang, Miniaturized Microstrip Wilkinson Power Divider With Harmonic Suppression, IEEE Microwave and Wireless Components Letters, vol.19, no.7, pp. 440-442, July 2009.
- J.P. Wang, B.Z. Wang, Y.X. Guo, L.C. Ong and S.Q. Xiao, A Compact Slow-wave Microstrip Branch-Line Coupler With High Performance, IEEE Microwave and Wireless Components Letters, vol.17, no.7, pp. 501-503, 2007.
- Y.X. Guo, Z.Y. Zhang, L.C. Ong, and M.Y.W. Chia, A novel LTCC miniaturized dualband balun, IEEE Microwave and Wireless Components Letters, vol. 16, no.3, March 2006, pp. 143-145.
- J. P. Wang, B.-Z. Wang, Y. X. Wang, and Y.-X. Guo, Dual-band microstrip stepped-impedance bandpass filter with defected ground structure, Journal of ElectroMagnetic Waves and Applications, vol.22, pp. 463-470, 2008.
- J. P. Wang, L. Wang, Y.X. Guo, Y.-X. Wang, and D. G. Fang, Miniaturized Dual-Mode Bandpass Filter with Controllable Harmonic Response for Dual-Band Applications, Journal of Electromagnetic Waves and Applications, vol. 23, pp. 1525-1533, 2009.
- J.P. Wang, L.J. Xu, S. Zhao, Y.X. Guo, W. Wu, Compact quasi-elliptic microstrip lowpass filter with wide stopband, Electronics Letters, vol. 46, no. 20, pp. 1384-1385, Sept 30 2010.
- G.L. Dai, Y.X. Guo, and M.Y. Xia, Dual-Band Bandpass Filter Using Parallel short-ended Feed scheme, IEEE Microwave and Wireless Components Letters, vol. 20, no.6, pp. 325-327, June 2010.
- G.L. Dai, Y.X. Guo, and M.Y. Xia, Design of a compact bandpass filter with improved selectivity using source-load coupling, Electronics Letters, vol. 46, no. 7, pp. 505-506, April 2010.
- Y.X Guo, L.C. Ong, M.Y.W. Chia, and B. Luo, Dual-band BPF in LTCC, IEEE MTT-S International Microwave Symposium, Long Beach, CA, June 12-17, 2005.
- J.P. Wang, L. Ge, Y.X. Guo, W. Wu, Miniaturized microstrip low-pass filter with broad stop-band and sharp roll-off, Electronics Letters, vol. 46, no.8, pp. 573-575, April 2010.

 156

Ka-Band SIW Quasi-Elliptic Filter

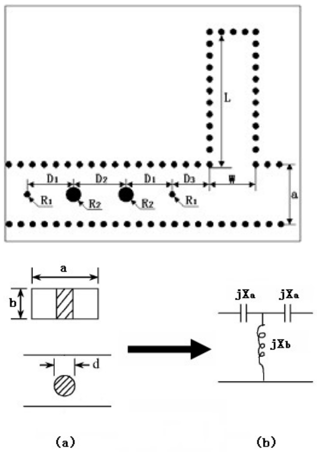

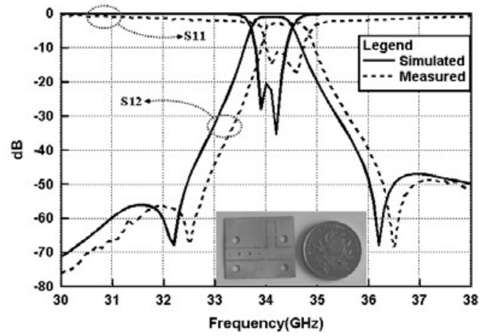

L. Bian, Y.X. Guo, and X.Q. Shi, Quasi-elliptic filter based on substrate integrated waveguide, Microwave and Optical Technology Letters, vol. 50, no.2, Feb 2008, pp. 402-404.

X-Band SIW Balun Filter (1/2)

Coupling schemes of a fifth-order bandpass filter

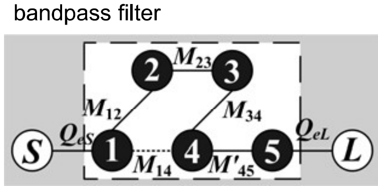

Coupling schemes of a sixth-order balun filter extended from the previous filter.

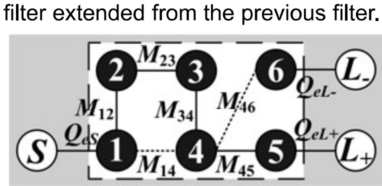

Synthesized frequency responses of the fifth-order bandpass filter and the sixth-order balun filter extended from it

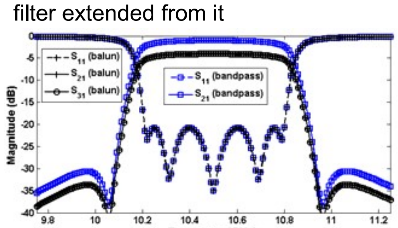

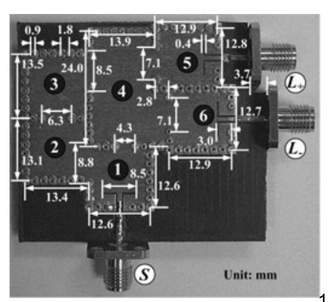

X-Band SIW Balun Filter (2/2)

Measured and simulated S-parameters

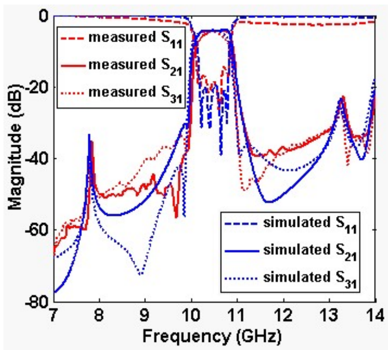

Measured balance of amplitude and phase

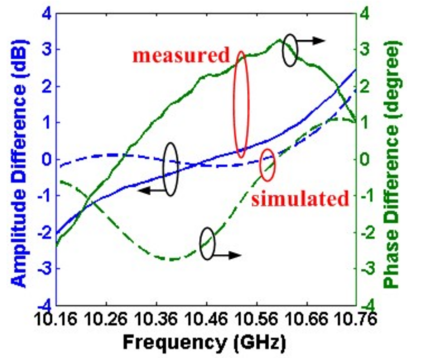

L.S. Wu, Y.X. Guo, J.F. Mao, W.Y. Yin, Design of a Substrate Integrated Waveguide Balun Filter Based on Three-Port Coupled-Resonator Circuit Model, IEEE Microwave and Wireless Components Letters, no.5, 2011

60-GHz LTCC SIW filter (1/2)

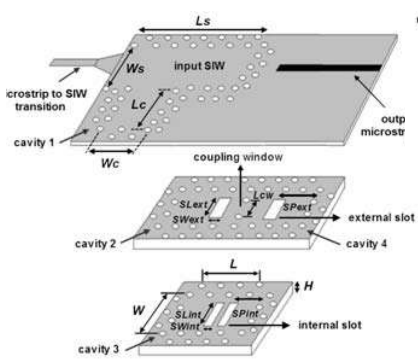

(a) 3-D overview

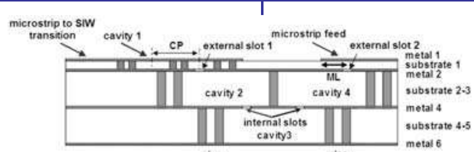

(b) side view

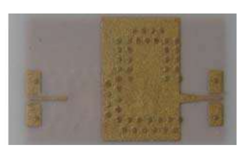

(c) photograph

H. Chu, Y.X. Guo, Y.Q. Shi, 60-GHz LTCC 3-D Cavity Bandpass Filter with Two Finite Transmission Zeros, Electronics Letters, vol. 47, No.5, 2011.

60-GHz LTCC SIW filter (2/2)

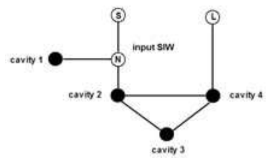

(d) Multi-coupling diagram

	S	1	N	2	3	4	L
S	0	0	2.3639	0	0	0	0
1	0	3.0818	6.3807	0	0	0	0
N	2.3639	6.3807	13.3624	1.9347	0	0	0
2	0	0	1.9347	-0.0102	0.6366	0.1338	0
3	0	0	0	0.6366	-0.2060	0.8688	0
4	0	0	0	0.1338	0.8688	-0.0102	1.088
L	0	0	0	0	0	1.088	0

(e) coupling matrix

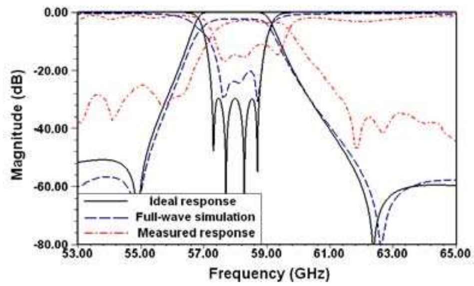

(f) Ideal circuit, simulated and measured responses

 161

40/50-GHz LTCC SIW Diplexer (1/2)

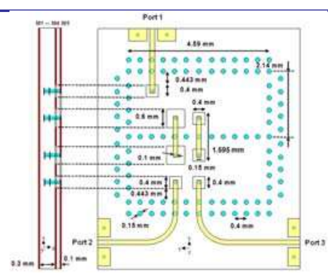

(a) Configuration and dimensions

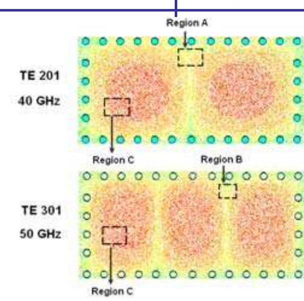

(b) Electric field patterns of and modes in single SIW cavity resonator

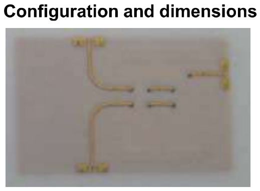

(c) Photograph

H. Chu, Y.X. Guo, Y.L. Song, Z.L. Wang, A novel 40/50 GHz diplexer design in LTCC technology, Electronics Letters, vol. 47, No.4, 2011

 162

40/50-GHz LTCC SIW Diplexer (2/2)

(d) Simulated S-parameter results

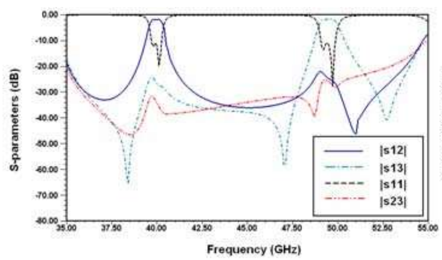

(e) Measured S-parameter results

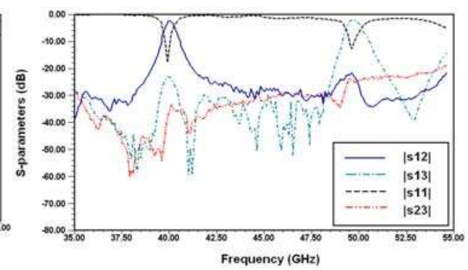

 163

LTCC UWB Filter

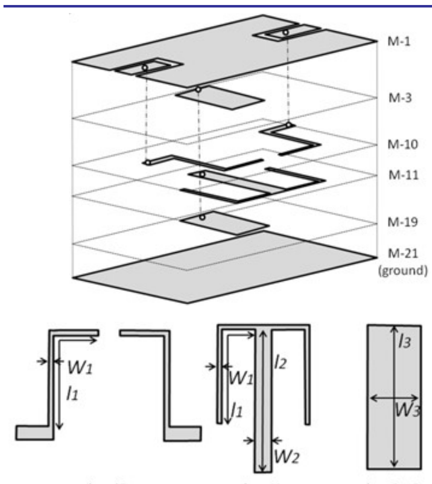

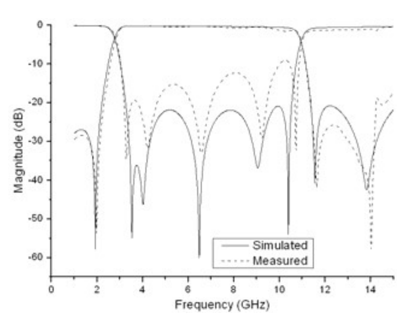

 164

LTCC UWB Notched Filter

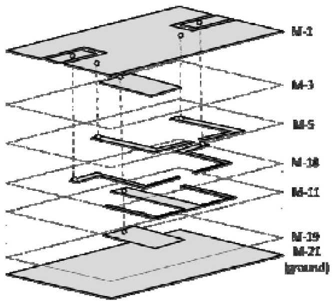

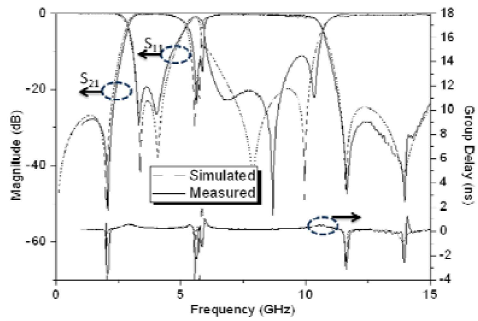

C.X. Zhou, Y.X. Guo, S.L. Yan, Z.L. Wang, Dual-band UWB filter with LTCC technology, Electronics Letters, vol.47, no.22, pp. 1230-1232, Oct 2011.

 165

Should you have any queries, please contact:

Dr. Yongxin Guo, Associate Professor
Department of Electrical and Computer Engineering
National University of Singapore
Email: eleguoyx@nus.edu.sg

 166